

Heterogeneous Causal Discovery of Repeated Undesirable Health Outcomes

SHISHIR ADHIKARI, University of Illinois Chicago, USA

GUIDO MUSCIONI, Anthem Inc., USA

MARK SHAPIRO, Carelon, USA

PLAMEN PETROV, Hydrogen Health, USA

ELENA ZHELEVA, University of Illinois Chicago, USA

Understanding factors triggering or preventing undesirable health outcomes across patient subpopulations is essential for designing targeted interventions. While randomized controlled trials and expert-led patient interviews are standard methods for identifying these factors, they can be time-consuming and infeasible. Causal discovery offers an alternative to conventional approaches by generating cause-and-effect hypotheses from observational data. However, it often relies on strong or untestable assumptions, which can limit its practical application. This work aims to make causal discovery more practical by considering multiple assumptions and identifying heterogeneous effects. We formulate the problem of discovering causes and effect modifiers of an outcome, where effect modifiers are contexts (e.g., age groups) with heterogeneous causal effects. Then, we present a novel, end-to-end framework that incorporates an ensemble of causal discovery algorithms and estimation of heterogeneous effects to discover causes and effect modifiers that trigger or inhibit the outcome. We demonstrate that the ensemble approach improves robustness by enhancing recall of causal factors while maintaining precision. Our study examines the causes of repeat emergency room visits for diabetic patients and hospital readmissions for ICU patients. Our framework generates causal hypotheses consistent with existing literature and can help practitioners identify potential interventions and patient subpopulations to focus on.

1 Introduction

An *undesirable outcome* is the occurrence of an unexpected or unwanted event associated with a negative impact on something of value. For example, serious illness, accidents, and traumas are undesirable outcomes associated with unpleasant human experiences. Undesirable outcomes may occur repeatedly and have a devastating impact. *Repeated undesirable outcomes* are the recurrences of unwanted events, such as repeat emergency room (ER) visits, hospital readmission, and relapse to addiction. Understanding the factors that trigger or prevent repeated undesirable outcomes is critical to designing intervention policies and mitigating the risk of future occurrences. In order for interventions to be effective, it is just as important to understand whether the causal factors have heterogeneous effects for different subpopulations and contexts. Focusing on heterogeneity enables the discovery of vulnerable subpopulations and designing interventions specific to them.

While repeated undesirable outcomes have been studied in the context of specific applications, such as recidivism [61], hospital readmissions [28] and ER visits [51], the solutions have been application-specific and have not considered heterogeneous causal discovery. In this paper, we formalize the problem of discovering heterogeneous causes of repeated undesirable outcomes and offer a novel application-agnostic framework for solving it. We motivate this problem with two real-world applications. The first one is the discovery of potential factors impacting repeat emergency room (ER) visits using patient medical claim data. Emergency rooms (or departments) are a critical part of a healthcare system for providing rapid access to care for patients with acute medical needs. ER overcrowding [49, 57] and overutilization of resources [4, 32], with estimated annual cost of nearly \$38 billion in the U.S. alone, have challenged clinicians and policymakers. One of the potential strategies to reduce this cost is better case management of patients with chronic diseases for preventing repeat ER visits [35].

Authors' Contact Information: Shishir Adhikari, sadhik9@uic.edu, University of Illinois Chicago, USA; Guido Muscioni, guido.muscioni@anthem.com, Anthem Inc., USA; Mark Shapiro, mark.shapiro@carelon.com, Carelon, USA; Plamen Petrov, plamen.petrov@khealth.com, Hydrogen Health, USA; Elena Zheleva, ezheleva@uic.edu, University of Illinois Chicago, USA.

We apply our methodology to identify causal factors of repeat ER visits of diabetic patients using a statistically de-identified dataset of 461,754 health insurance claims from a large insurance company. Although medical claims of patients are administrative records for billing the insurance company, they also contain important clinical information, such as the patient's diagnosis or relevant medical history (e.g., smoking habit) across multiple facilities. The second application is that of discovering factors that trigger or inhibit hospital readmissions using electronic health record (EHR) data. Hospital readmissions incur high healthcare expenses. The hospital readmission rate is transparent under the Affordable Care Act [46] and reflects the quality of care affecting the hospital's reputation. Hospitals with excessive unplanned readmission rates are subjected to penalties [10]. Although hospital readmission is known to be linked to complications during admission, comorbidities, quality of care in hospital, and post-discharge situations [28], understanding heterogeneous causes of hospital readmissions is useful for designing effective interventions. We apply our methodology to identify causal factors of hospital readmissions using 335,378 admission records in the Medical Information Mart for Intensive Care (MIMIC)-IV [24] dataset.

This paper examines the opportunities and challenges to address heterogeneous causal discovery by building upon the ideas of causal discovery [55], characterization of effect modifiers [60], and identification of heterogeneous effects [40, 41]. We propose an end-to-end *heterogeneous causal discovery framework* for discovering interventions that can decrease undesirable outcomes and work for heterogeneous subpopulations. The first novel part in our framework is an ensemble of causal structure learning algorithms that discovers and assigns support to potential causes. The second novel part is the discovery of effect modifiers and estimation not only of total causal effects but also heterogeneous causal effects. This allows the discovery of interventions that can be tailored to different subpopulations. Specifically, we discover which diagnosis codes in patients' claims or health records preceding the repeat ER visits or hospital readmissions are potential causes of the recurrence. By quantifying the magnitude, and heterogeneity of causal effects, our framework enables two main venues of intervention planning. First, diagnosis codes with large positive causal effects correspond to subpopulations of patients that should be prioritized for interventions. Second, diagnosis codes with negative causal effects can be studied as potential interventions. Because of the task novelty and the lack of causal ground truth in real-world data, we validate the discovered heterogeneous causes through existing research literature. We also evaluate our framework using simulated data in which ground truth is available.

In summary, the overall contribution of our research is threefold. First, from a research problem perspective, we investigate a novel problem of jointly discovering causes and effect modifiers triggering or preventing an outcome under the uncertainty of the underlying data generating mechanism. Second, from a methodological perspective, to the best of our knowledge, this is the first work to propose and evaluate the use of an ensemble of causal structure learning (CSL) algorithms to generate cause-and-effect hypotheses with confidence measures. Third, from a real-world impact perspective, we showcase the applicability of our framework in discovering causes and effect modifiers triggering or preventing repeat ER visits and hospital readmissions.

Next, we present background and related work. We formulate the problem of discovering causes and effect modifiers in §4, and discuss opportunities and challenges of addressing the problem with observational data in §5. Sections 6 and 7 present our methodology and experimental evaluations before concluding the paper.

2 Related Work

Analysis of repeat ER visits and hospital readmissions. There are multiple studies on identifying the factors contributing to repeat ER visits and readmissions, including meta-analyses [30, 51, 54], retrospective observational studies [16, 23], prospective cohort studies [36, 48], and PRISMA-based root cause analysis [12, 13, 59]. The PRISMA (Prevention and Recovery Information System for Monitoring and Analysis) method involves trained investigators manually constructing a causal tree after systematic interviews with the patients. There is a growing

interest in identifying and analyzing heterogeneous subpopulations associated with recurrent ER visits and readmissions by utilizing observational and interventional data [6, 42, 54]. Our approach uses retrospective observational data for large-scale automatic discovery of potential causes and sources of heterogeneity to assist investigators in identifying and designing interventions.

Causal discovery in healthcare domains. Causal discovery approaches have been employed in healthcare domains, utilizing different background information. Wang et al. [62] have used local causal structure learning with prior domain knowledge for discovering causal relationships between Type 2 Diabetes and Bone Mineral Density (BMD) related conditions. A recent approach [22] has utilized prior knowledge extracted from multiple Authoritative Medical Ontologies (AMO) to orient edges learned from a causal Bayesian learning algorithm. Nordon et al. [37] used causal relations extracted from medical literature to construct a causal graph and electronic medical record (EMR) data to prune the edges with no correlation. Our approach utilizes an ensemble of causal discovery algorithms with the background knowledge that the patient outcome (e.g., readmission) is never a parent of other contexts (diagnosis codes) due to the temporal order of occurrence.

Causal structure learning approaches. Causal structure learning (CSL) algorithms can be classified into four types according to their approach: (1) constraint-based, (2) scored-based, (3) hybrid, and (4) functional causal model-based. The idea for CSL is to utilize conditional independencies (CI) in the data distribution to infer the structure of the causal graphical model. The notion of *d-separation* [39, 40] is used to read off all CI that hold for any data distribution that is generated by the mechanism described by a graphical model. The same conditional independence relation can be satisfied by multiple causal models belonging to a Markov equivalence class, and CSL generally concerns learning a Markov equivalence class. Constraint-Based algorithms, such as PC [11, 55] and Fast Causal Inference (FCI) [55], use conditional independencies in the data as constraints to estimate an equivalence class of underlying SCM. Score-based algorithms, such as Greedy Equivalence Search (GES) [8] and Fast GES [47], consider causal structure learning as the problem of fitting a CPDAG to the data according to a relevant score function that relates to how well the CPDAG captures the conditional independencies in the data. Hybrid algorithms combine both constraint-based and score-based approaches. Max-Min Hill Climbing (MMHC) [58] uses a constraint-based Max-Min Parents and Children (MMPC) local discovery algorithm for skeleton determination and a score-based Hill-Climbing (HC) [50] for edges orientation. The functional causal models [17] use SCM with additional assumptions on the distribution of U and V to distinguish between different DAGs in the same equivalence class. Recently, methods using continuous optimization [64, 65] are popular for extracting a directed acyclic graph (DAG) structure from observational data. Although these gradient-based techniques are scalable, the output DAG lacks a causal interpretation and these methods are less reliable with real-world data [25]. The CSL algorithms and their assumptions with empirical performances have been reviewed with a continuous data [21]. Previous work on causal effect estimation combining CSL and covariate adjustment focused on identifying a multi-set of causal effects for the equivalence class of a single DAG [31, 44]. Here, we study the behavior of CSL algorithms and their ensemble with categorical non-linear data for discovering causes and effect modifiers of a sink outcome node.

There are approaches [18] for causal discovery using event sequences that may seem more relevant for medical claims data or electronic health records. These algorithms rely on the crucial assumption that a cause precedes an effect temporally. The diagnosis of diseases may not reflect the true order of occurrence of diseases. For example, disease A may lead to disease B but the diagnosis of disease B might be earlier than that of disease A. Therefore, we do not utilize causal discovery using event sequences in this work and instead rely on the aggregation that only considers the historical presence or absence of diagnosis codes for a patient leading to the observed outcome.

3 Preliminaries

3.1 Structural Causal Model (SCM)

A SCM $\mathcal{M}(\mathbf{V}, \mathbf{U}, \mathbf{f})$ models the underlying data-generating mechanism with a set of exogenous variables \mathbf{U} , endogenous variables \mathbf{V} , and functions \mathbf{f} . A variable is a function of its known direct causes and unknown disturbances. The causal relationship among the variables in an SCM is represented using a directed acyclic graph (DAG) $G(\mathbf{V}, \mathbf{E})$ where \mathbf{V} and \mathbf{E} are a set of vertices and edges, respectively, and each vertex has incoming edges from its direct causes. $V_i \rightarrow V_j$ denotes an edge from the parent V_i to the child V_j . Two vertices are adjacent if there is an edge between them. A directed path is a sequence of nodes obtained following the direction of the edges. A graph is directed acyclic if there are no directed paths with repeated nodes. The nodes preceding the tail node of the directed path are the ancestors of the tail node. The nodes following the head node of the directed path are descendants of the head node. The symbols $pa(V_i, G)$, $anc(V_i, G)$, and $des(V_i, G)$ indicate the sets of parents, ancestors, and descendants of V_i for graph G , respectively. Given a ground truth G , the causes of an outcome Y are its ancestors.

3.2 Effect modifier (EM)

Although the presence of effect modification is determined by the estimation of CATE (Eq. 5), the graphical structure G can still inform about potential interactions that results in effect modification. VanderWeele and Robins [60] use DAGs to categorize four types of potential effect modifiers: direct, indirect, common cause, and proxy. All effect modifiers are non-descendants of the treatment and outcome. Direct EMs are the parents of the outcome except the treatment. Indirect, common cause, and proxy EMs are related to the direct EM by ancestor, confounding, and descendant relationships, respectively. In general, the potential interacting variables for a given treatment and outcome in a G include the non-descendants of the treatment node and either (1) the parents of the outcome or (2) the parents of mediator nodes in the directed path from treatment to outcome [60].

3.3 Conditional Average Treatment Effect (CATE) Identification

The cause-and-effect hypotheses encoded in G can be used to identify causal effects from observation data using do-calculus [40]. Here, we show backdoor adjustment [40] for the identification of causal effects. Let \mathbf{W} be an adjustment set such that $\mathbf{W} \cup \mathbf{Z}$ satisfies the backdoor criterion for treatment X , outcome Y , and contexts \mathbf{Z} . The interventional distributions $E[Y|do(X = x), \mathbf{Z} = \phi]$ and $E[Y|do(X = x), \mathbf{Z} = \mathbf{z}]$ can be estimated, respectively, in terms of observational distribution with backdoor adjustment as:

$$\begin{aligned} E[Y|do(X = x), \mathbf{Z} = \phi] &= \sum_{\mathbf{w}} E[Y|X = x, \mathbf{W} = \mathbf{w}]P(\mathbf{W} = \mathbf{w}), \text{ and} \\ E[Y|do(X = x), \mathbf{Z} = \mathbf{z}] &= \sum_{\mathbf{w}} E[Y|X = x, \mathbf{W} = \mathbf{w}, \mathbf{Z} = \mathbf{z}]P(\mathbf{W} = \mathbf{w}|\mathbf{Z} = \mathbf{z}). \end{aligned} \quad (1)$$

To satisfy backdoor criteria, \mathbf{W} should not be descendants of X and $\mathbf{W} \cup \mathbf{Z}$ should block all backdoor paths from X to Y . These estimands can be substituted in Equation 4 to estimate CATE.

3.4 Causal Structure Learning (CSL)

The idea for CSL is to utilize conditional independencies (CI) in the data distribution to infer the structure of the causal graphical model. The joint distribution P described by $G(\mathbf{V}, \mathbf{E})$ factorizes to the product of the conditional probability of each random variable given its parents according to causal Markov assumption, i.e., $P(V_1, \dots, V_n) = \prod_{i=1}^n P(V_i|pa(V_i, G))$. The notion of *d-separation* [39, 40] is used to read off all CI that hold for any data distribution that is generated by the mechanism described by a graphical model. The same conditional independence relation can be satisfied by multiple causal models belonging to a Markov equivalence class, and CSL generally concerns learning a Markov equivalence class. Additional parametric assumptions and background knowledge are needed to identify a causal model within the equivalence class. We summarize four categories

of causal structure learning algorithms according to their approach: (1) constraint-based, (2) scored-based, (3) hybrid, and (4) functional causal model-based. Constraint-Based algorithms, such as PC [11, 55] and Fast Causal Inference (FCI) [55], use conditional independencies in the data as constraints to estimate an equivalence class of underlying SCM. The PC algorithm makes assumptions of causal sufficiency and faithfulness for the correctness of edge adjacencies. Then, v-structure discovery followed by Meek orientation rules [33] produces an equivalence class graph, also known as a completed partial directed acyclic graph (CPDAG). FCI is also a constraint-based algorithm that relaxes the causal sufficiency assumption of PC algorithm. FCI outputs a partial ancestral graph (PAG), a Markov equivalence class of maximal ancestral graph (MAG), to incorporate the hidden confounders using a bidirectional arrow, i.e., $V_i \leftrightarrow V_j$. In a PAG, $V_i \rightarrow V_j$ is interpreted as V_i being an ancestor of V_j and V_j not being an ancestor of V_i . Similarly, $V_i \circ \rightarrow V_j$ indicates either V_i is an ancestor of V_j and/or there is a hidden confounder between V_i and V_j , but V_j is not an ancestor of V_i .

Score-based algorithms, such as Greedy Equivalence Search (GES) [8] and Fast GES [47], consider causal structure learning as the problem of fitting a CPDAG to the data according to a relevant score function that relates to how well the CPDAG captures the conditional independencies in the data. FGES's implementation in `py-causal` [63] package provides some robustness to faithfulness assumption. These algorithms assume causal sufficiency. Under the fulfilment of assumptions and infinite sample size with absence of selection bias, both PC and GES algorithms are shown to be sound and complete.

Hybrid algorithms combine both constraint-based and score-based approaches. Max-Min Hill Climbing (MMHC) [58] uses a constraint-based Max-Min Parents and Children (MMPC) local discovery algorithm for skeleton determination and a score-based Hill-Climbing (HC) [50] for edges orientation. GFICI [38] is a hybrid algorithm that relaxes causal sufficiency assumption.

The functional causal models [17] use SCM with additional assumptions on the distribution of \mathbf{U} and \mathbf{V} to distinguish between different DAGs in the same equivalence class. Linear Non-Gaussian Acyclic Model (LINGAM) [52] assumes causal sufficiency, linear data generating process, and exogeneous variables with Non-Gaussian distributions of non-zero variance. Although additive noise models for discrete data have been proposed, it is too restrictive for binary variables [45]. Recently, methods using continuous optimization [64, 65] are popular for extracting a DAG structure from observational data. However, these methods performed poorly on our synthetic data and we excluded them from our analysis.

4 Problem Setup

First, we present our data model to represent and abstract patient data used in our study. Then, we formally describe the problem of discovering the causes and effect modifiers of patient outcomes.

4.1 Data Model

Event-log data model. Let $e_{i,t}^j \in \{0, 1\}$ and $o_{i,t} \in \{0, 1\}$ represent an event of interest of type e^j and an undesirable outcome o for unit i at time t . We consider M events $e^j \mid j \in \{1, \dots, M\}$ that are potentially related to the undesirable outcome o . The binary values 1 and 0, respectively, indicate the presence and the absence of the events or a outcome for a given unit and time. Each independent unit consists of a timeline $E_i \in \{0, 1\}^{(M+1) \times T}$ of time frame T consisting of events and outcomes.

Figure 1 illustrates the data model described above for N units and $M = 3$ events with one undesirable outcome. For visual conciseness, a sparse representation of event vectors is shown with events $\{e^j \mid e_{i,t}^j = 1\}$. The triangle, square, and diamond shapes represent different event types that are potentially related to the undesirable outcome depicted with a circle. The shaded figures indicate the presence of an event. In context to the real-world use case in our study, the undesirable outcome is an ER visit. The events can include diagnoses of diseases, routine office visits, or encounters of immunization. We refer to this data model as *event-log data model*.

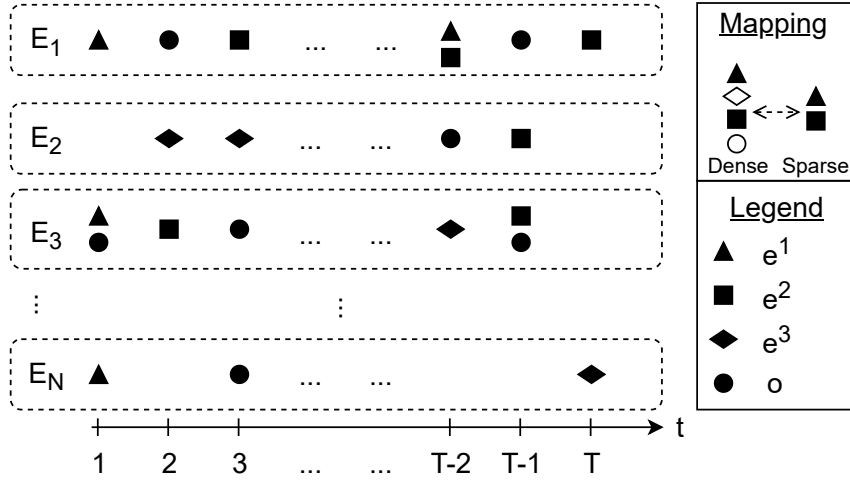


Fig. 1. Illustration of data model with timeline $E \in \{0, 1\}^{4 \times T}$ for N units with three endogenous events (e^1 , e^2 , and e^3) and an undesirable outcome (o).

Each unit i or event at a timepoint t can have covariates, X_I or X_T , respectively. For example, for our use case on readmission, we incorporate socio-demographic covariates describing a patient (unit), and temporal contextual covariates describing a hospitalization event. Next, we define the population of interest and the repeated undesirable outcome using the event-log data model.

Population of interest. Our population of interest (P) consists of units with at least one undesirable outcome. Formally, the population is a subset of units such that there exists at least one undesirable outcome in the unit's timeline i.e. $P \subseteq E \mid \forall E_i \in P, \exists t \in \{1, \dots, T\}, o_{i,t} = 1$.

Repeated undesirable outcome. If an undesirable outcome recurs within a specified time interval τ of the prior undesirable outcome, then the more recent outcome is a repeated undesirable outcome. Let, $t' \in \{t+1, \dots, T\} \cup \emptyset$ indicate the time point of the undesirable outcome occurring after a reference time point t in which there was an undesirable outcome $o_{i,t} = 1$, and is defined as follows:

$$t' := \min(p \in \{t+1, \dots, T\} \mid o_{i,p} = 1), \quad (2)$$

where \emptyset indicates a null value.

The repeated undesirable outcome $y_i(t, t', \tau) \in \{0, 1\}$ is defined by the specified time interval τ , the reference time point t , and the time point t' :

$$y_i(t, t', \tau) := \begin{cases} 0 & \text{if } t' = \emptyset \\ 0 & \text{if } t' - t > \tau \\ 1 & \text{if } t' - t \leq \tau \end{cases} \quad (3)$$

Equation (3) enables mapping of multiple occurrences of undesirable outcomes at time points $t \in \{1, \dots, T\} \mid o_{i,t} = 1$ to a binary value representing a *repeated* undesirable outcome i.e. $y_i(\tau) = 1$ if $\exists t, y(t, t', \tau) = 1$ and 0 otherwise. Moving forward, we use the terms "outcome" and "repeated undesirable outcome" interchangeably.

For example, let us consider the timeline E_3 in Figure 1. If the time interval $\tau = 2$, then the outcome is $y_3(1, 3, 2) = 1$ because the consecutive undesirable outcomes are within the specified time interval. However, if we consider $\tau = 1$ for the timeline E_3 , the outcome is $y_3(1, 3, 1) = 0$. We treat the value of τ to be domain-specific and available from standard practice or domain experts. The commonly used interval for hospital readmission is 30 days [3] and for recidivism is three years [34].

4.2 Discovering causes and effect modifiers

In this section, we first describe the causes and effect modifiers of an outcome using hypothetical interventional distribution [40] and then formally define our research problems.

Under stable unit treatment value assumption (SUTVA), a variable X is a cause of outcome Y if the *conditional average treatment effect* (CATE) for any context $\mathbf{Z} = \mathbf{z}$ is non-zero, i.e.,

$$\exists \mathbf{z}, X_{CATE}(\mathbf{Z} = \mathbf{z}) := E[Y|do(X = x), \mathbf{Z} = \mathbf{z}] - E[Y|do(X = x'), \mathbf{Z} = \mathbf{z}] \neq 0, \quad (4)$$

where $do(X = x)$ and $do(X = x')$ denote interventions to the value of X with policies x and x' , respectively. We assume the context \mathbf{Z} is not affected by the outcome to ensure the soundness of CATE estimand. The causal effect in Equation 4 is measured on a difference scale but sometimes, for a binary outcome, the effect may be measured on a multiplicative scale like a risk ratio or an odds ratio. A treatment may have heterogeneous effects on the outcome in different contexts. These contexts are referred to as effect modifiers. A set of variables \mathbf{Z} are effect modifiers for treatment X and outcome Y if CATE is different for any two contexts \mathbf{z} and \mathbf{z}' that are instances of \mathbf{Z} , i.e.,

$$X_{CATE}(\mathbf{Z} = \mathbf{z}) \neq X_{CATE}(\mathbf{Z} = \mathbf{z}'). \quad (5)$$

Next, we formally define two research problems.

Problem 1 (*Discovering causes of an outcome*) Given a set of variables \mathbf{X} and the outcome Y , find a set of variables $\{X \in \mathbf{X} | \exists \mathbf{z}, X_{CATE}(\mathbf{Z} = \mathbf{z}) \neq 0\}$.

Problem 2 (*Discovering effect modifiers of a treatment and an outcome*) Given a treatment X and outcome Y , find all contexts $\{\mathbf{z}, \mathbf{z}'\} \in \mathbf{Z} \subset \mathbf{X} \setminus \{X, Y\}$ such that Equation 5 holds.

The magnitude and sign of $X_{CATE}(\mathbf{Z} = \mathbf{z})$ help to distinguish whether causes and effect modifiers are triggering or preventing the outcome. An effect modifier Z for a treatment may or may not be a cause of the outcome. We refer to the causes and causal effect modifiers as *heterogeneous causes* of the outcome and focus on discovering them. Identification of causal effect modifiers can help in effective targeted interventions.

5 Discovering Causes and Effect Modifiers from Observational Data

The research problems described in §4 are defined in terms of interventional distributions. Here, we discuss the opportunities and challenges for addressing the research problems with observational data using the ideas of the structural causal model [40] and causal structure learning [55].

Effect modifier (EM). Although the presence of effect modification is determined by the estimation of CATE (Eq. 5), the graphical structure G can still inform about potential interactions that results in effect modification. VanderWeele and Robins [60] use DAGs to categorize four types of potential effect modifiers: direct, indirect, common cause, and proxy. All effect modifiers are non-descendants of the treatment and outcome. Direct EMs are the parents of the outcome except the treatment. Indirect, common cause, and proxy EMs are related to the direct EM by ancestor, confounding, and descendant relationships, respectively. In general, the potential interacting variables for a given treatment and outcome in a G include the non-descendants of the treatment node and either (1) the parents of the outcome or (2) the parents of mediator nodes in the directed path from treatment to outcome [60].

CATE identification. The cause-and-effect hypotheses encoded in G can be used to identify causal effects from observation data using do-calculus [40]. Here, we show backdoor adjustment [40] for the identification of causal effects. Let \mathbf{W} be a adjustment set such that $\mathbf{W} \cup \mathbf{Z}$ satisfies the backdoor criterion for treatment X , outcome Y , and contexts \mathbf{Z} . The interventional distributions $E[Y|do(X = x), \mathbf{Z} = \phi]$ and $E[Y|do(X = x), \mathbf{Z} = \mathbf{z}]$ can be estimated, respectively, in terms of observational distribution with backdoor adjustment as:

$$\begin{aligned} E[Y|do(X = x), \mathbf{Z} = \phi] &= \sum_{\mathbf{w}} E[Y|X = x, \mathbf{W} = \mathbf{w}]P(\mathbf{W} = \mathbf{w}), \text{ and} \\ E[Y|do(X = x), \mathbf{Z} = \mathbf{z}] &= \sum_{\mathbf{w}} E[Y|X = x, \mathbf{W} = \mathbf{w}, \mathbf{Z} = \mathbf{z}]P(\mathbf{W} = \mathbf{w}|\mathbf{Z} = \mathbf{z}). \end{aligned} \quad (6)$$

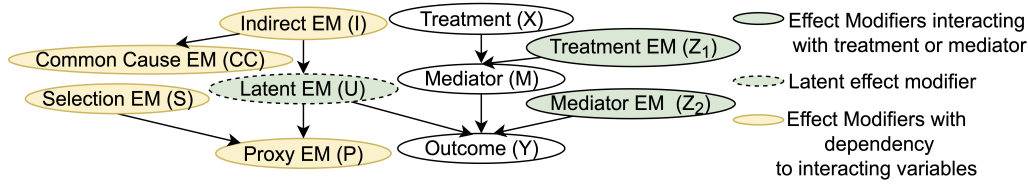


Fig. 2. Characterization of effect modifiers (EM) with a structural causal model (SCM).

To satisfy backdoor criteria, \mathbf{W} should not be descendants of X and $\mathbf{W} \cup \mathbf{Z}$ should block all backdoor paths from X to Y . These estimands can be substituted in Equation 4 to estimate CATE.

5.1 Characterization of Effect Modifiers with SCM

Here, we characterize effect modifiers with SCM. In general, effect modification is induced due to the presence of direct interactions between context $Z \in \mathbf{Z}$ and treatment X in the underlying function that defines outcome Y , e.g., $Y = f_Y(g(X) \times h(Z))$, where $f_Y \in \mathbf{f}$, g and h are feature mapping functions, and \times denotes interaction. In the above example, the causal effect of X on Y can be estimated by taking a partial derivative of Y with respect to X , i.e., $\frac{\partial Y}{\partial X} = f'_Y(\cdot)h(Z)g'(X)$, where the causal effect of X on Y varies depending on $h(Z)$. The non-linearity of the function f_Y can introduce heterogeneity, due to the term $f'_Y(\cdot)$, even when there is no direct interaction. For example, if $Y = e^{3X+Z}$, then $\frac{\partial Y}{\partial X} = 3e^{3X+Z}$, with $f'_Y(\cdot) = e^{3X+Z}$ indicating variability in causal effects depending on Z . We refer the heterogeneity due to non-linearity of functions as indirect interaction.

Figure 2 summarizes our characterization of effect modifiers, adapted from VanderWeele and Robins [60], based on interactions and dependencies in G : (1) effect modifiers (EM) interacting with treatment or mediator, (2) latent EM, and (3) EM with dependency to interacting variables. A shared child node in G may result in a direct or indirect interaction. While mediator EMs only share a child (M or Y) with mediators and not treatment directly, treatment EMs share a child (M or Y) with treatment. These interacting variables could be latent, either known or unknown. As shown in Figure 2, indirect, proxy, common cause, and selection effect modifiers are non-descendants of treatment with dependence to interacting variables via ancestor, descendant, confounding, and selection (or spouse) relationships, respectively. In Figure 2, only the effect modifiers Z_1 , Z_2 , and I are causal effect modifiers, while the others (P , S , and CC) are non-causal.

5.2 Opportunities and Challenges

A natural approach to addressing Problem 1 is to learn a $G(\mathbf{V}, \mathbf{E})$ to find causes and Problem 2 is to identify potential effect modifiers, and then test the presence of heterogeneous effects. Causal structure learning (CSL) [55] concerns learning the adjacency and the orientation of the edges in G using observational data and, optionally, background knowledge. Some CSL algorithms like FCI [55] can even detect presence of latent confounding. However, to infer a causal structure without accessing interventional distribution, CSL methods must make assumptions about the unknown underlying data generating mechanism. Causal sufficiency and faithfulness are the main assumptions made by CSL algorithms for estimating correct adjacencies and orientations of edges. These assumptions may be relaxed by some CSL algorithms. *Causal sufficiency* assumes that there are no unmeasured common causes of variables in \mathbf{V} . *Faithfulness* assumes all the conditional independencies (CI) observed from the data are entailed by the d-separation conditions [39] of an underlying G .

In our problem, violation of the causal sufficiency can lead to false causes and non-identifiability of effect modification. For example, in Figure 2, with unobserved U , the proxy effect modifier P may be falsely discovered as a cause of Y and a causal effect modifier. Even though our proposed framework is general enough that it can include CSL algorithms that allow for latent variables, for simplicity of exposition, we focus on ones that

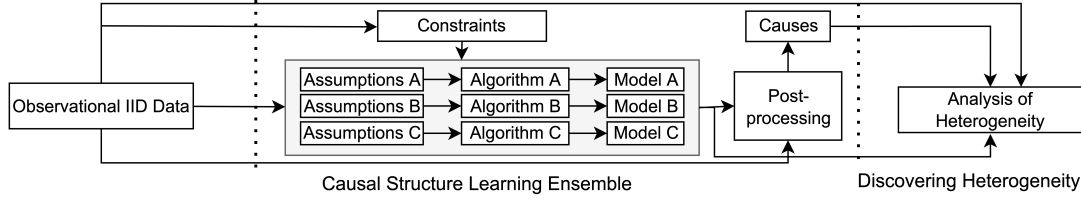


Fig. 3. Heterogeneous causal discovery framework.

assume causal sufficiency. Due to heterogeneity, data distribution may have more CI relations than those implied by G , resulting in a violation of faithfulness assumption. For example, a collider structure $X \rightarrow Y \leftarrow Z$ with binary $X = \theta(0.6)$, $Z = \theta(0.5)$, and $Y = \theta(0.4 + 0.2X + 0.24Z - 0.4XZ)$ has an unfaithful distribution. Here, $E[\frac{\partial Y}{\partial X}]$ and $E[\frac{\partial Y}{\partial Z}]$ are both zero making both X and Z marginally independent of Y although X and Z are causes of Y . Although unfaithfulness due to counterbalancing parameters is rare [55], sufficient sample size and absence of selection bias is desired in practice for faithful distributions. CSL methods may rely on CI tests, goodness-of-fit scores, and cause-effect asymmetries making additional parametric assumptions about the nature of the functions in SCM [17].

We focus on discovering causes and causal effect modifiers of the outcome. The data for our use cases is largely binary indicating presence or absence of a disease or an event. Without loss of generality, we concentrate on non-linear categorical data generating mechanisms. One important difficulty in CSL is the uncertainty of a model's assumptions being violated when the assumptions are untestable with data. Causal sufficiency, faithfulness, acyclicity, and absence of selection bias are mostly untestable. For our use case with largely binary variables, parametric assumptions like additive noise models are too restrictive or unsuitable [45]. CSL algorithms may be sensitive to the number of nodes, the sparsity of edges, underlying network topology, and the strength of causal effects. We hypothesize an ensemble of CSL algorithms can mitigate this issue by discovering causes that persist across different assumptions. Here, we test whether multiple CSL algorithms in an ensemble agree on actual causes and make dissimilar mistakes for false causes and test the utility of an ensemble for ranking causes based on confidence scores. While careful model selection is desirable, we lack a clear metric to identify a correct model from others under untestable assumptions and absence of ground truth. We rely on empirically evaluating the CSL ensemble using simulated data. Theoretical support for the CSL ensemble approach is not trivial because the potential causes are not independent of one another.

6 Heterogeneous Causal Discovery Framework

Figure 3 presents a high-level overview of our proposed methodology for discovering heterogeneous causes, i.e., causes and causal effect modifiers, that are responsible for triggering or preventing the outcome. The framework takes independent and identically distributed (IID) observational data as an input. Then, an ensemble of CSL algorithms is employed to learn causal graphical models, which are used to discover prominent causes that trigger or prevent the outcome. Finally, the module for heterogeneity analysis takes the discovered causes, observational data, and causal models to discover the effect modifiers of the outcome together with heterogeneous effects estimates. The data consists N records of observed variables $\mathbf{X} \in \mathbb{B}^{N \times M}$ and the outcome $Y \in \mathbb{B}^N$.

6.1 Causal Structure Learning Ensemble

Problem 1 of discovering causes, described in §4, translates to learning $G(\mathbf{V}, \mathbf{E})$ with vertices $\mathbf{V} = \mathbf{X} \cup \{Y\}$, and then answering $anc(Y, G)$ query. This module takes observational data and *structural constraints* as inputs. The CSL ensemble module outputs a list of causes and *cause support* metric as a measure of confidence for each cause.

Structural constraints. Structural constraints are optionally used by CSL algorithms to encode background knowledge. We assume that the variables \mathbf{X} are measured prior to the outcome Y . This is a reasonable assumption

in real-world use cases. For instance, the diagnosis codes encountered prior to repeat ER visits are considered as potential causes. This also ensures the soundness of the CATE estimand, as discussed in §4. Therefore, we include a structural constraint that the outcome Y is never a parent, i.e., $\forall V_j | E(V_i \rightarrow V_j) \in \mathbf{E}, Y \notin pa(V_j, G)$.

Cause support. The CSL ensemble takes the data and constraints as inputs to multiple CSL algorithms with possibly different causal assumptions or methodologies, and outputs DAG or equivalence classes (see Appendix A) of DAGs. The constraints aid in the orientation of edges adjacent to Y as well as the orientation of undirected edges in the equivalence class. To obtain causes of the outcome Y , we iterate through all K output causal graphs and find tuples of a variable and a graph such that the variable is an ancestor of the outcome in the graph i.e. $\mathbf{R} := \{(X_j, G_k) \mid \exists G_k \in \{G_1, \dots, G_K\}, X_j \in anc(Y, G_k) \wedge X_j \in \mathbf{X}\}$. The cause support for a cause X_j shows the fraction of final K graphs, one per CSL algorithm, that contain X_j as a cause of outcome Y , and is defined as $S_c(X_j) = \frac{1}{K} \sum_k \#[(X_j, G_k) \in \mathbf{R}]$, where $\#[.]$ is an indicator variable.

6.2 Discovering heterogeneity

This module takes the observational data, K output graphs, and the set \mathbf{R} consisting of the tuples of a cause with a pointer to the corresponding graph as inputs.

Total effect estimation. We estimate the average total causal effect (ATE) $X_{jCATE}(Z = \phi)$ for each pair of $(X_j, G_k) \in \mathbf{R}$ using backdoor adjustment set $\mathbf{W} = pa(X_j, G_k)$, if identifiable. Nonparametrically, the ATE is calculated by substituting Equation 6 into Equation 4 and calculating the expectations and probability distributions. This approach maybe computationally expensive and, in practice, ATE can be estimated by regressing Y on treatment and adjustment set $\{X_j\} \cup \mathbf{W}$ with any suitable machine learning model. We use a linear model to obtain ATE and its statistical significance utilizing the regression coefficient and p-value of X_j .

Identifying effect modifiers. The module for analysis of heterogeneity, shown in Figure 3, involves short-listing potential effect modifiers (EM), for a given treatment X_j and outcome Y , together with estimation of the heterogeneous and average total treatment effects across causal models $\{G_1, \dots, G_K\}$. Let $G_k^{anc}(\mathbf{V}^{anc}, \mathbf{E}^{anc}) \mid V^{anc} \in \{Y\} \cup anc(Y, G_k)$ denote a sub-graph of G_k with Y , $anc(Y, G_k)$, and edges between them retained. Given a graph G_k , treatment X_j , and outcome Y , the potential treatment EM and mediator EM, as described in §5, are tuple of node and graph pair $\mathbf{Z} := (Z_i, G_k) \mid Z_i \notin des(X_j, G_k^{anc}) \wedge \exists V_d \in des(X_j, G_k^{anc}), Z_i \in pa(V_d, G_k^{anc})$.

Estimating heterogeneous treatment effects (HTE). We check the presence of actual heterogeneity for treatment X_j , outcome Y , and potential effect modifier $(Z_i, G_k) \in \mathbf{Z}$ following Equation 5. The estimation of CATE uses backdoor adjustment set \mathbf{W} conditioned on $Z_i = z$. Similar to ATE, the HTE is estimated nonparametrically or by regressing Y on $\{X_j, Z_i, Z_i \times X_j\} \cup \mathbf{W} \cup \{\mathbf{W} \times Z_i\}$, where $Z_i \times X_j$ is an interaction term between treatment and conditional variable and $\mathbf{W} \times Z_i$ captures interactions between adjustment set and conditional variable. Using a linear regression model with interaction terms, we can detect the presence of a heterogeneous effect with a statistically significant non-zero coefficient for the interaction term. Here, we demonstrate identifying heterogeneity using a linear model with pairwise interaction terms. However, the variables $\{X_j, Y, \mathbf{W}, \mathbf{Z}\}$ can be used with any HTE estimator [2, 29] to discover more complex subpopulations.

The final output of the framework includes the following: (1) for an observational dataset and an outcome, a list of causes with causal support and a multi-set of their average total causal effects, and (2) for a given cause and outcome, a list of effect modifiers with causal support and a multi-set of heterogeneous treatment effects.

7 Experiments

We conduct experiments to evaluate the proposed framework for discovering causes and sources of heterogeneity for an outcome in two ways. First, using real-world data, we demonstrate the top causes triggering or preventing the outcome, discovered by our approach, are consistent with the published research literature. Second, we evaluate the significance of the ensemble approach using synthetic and semi-synthetic data.

7.1 Real-World Application

Here, we describe the real-world dataset and experimental setup for discovering heterogeneous causes of repeat ER visits. We present the results summarizing discovered causes and effect modifiers for some potential interventions. Because of the task novelty and the lack of ground truth in our data, we validate the discovered heterogeneous causes through published medical research. We also tested large language models (LLMs), like ChatGPT, to verify the discovered cause-effect hypotheses. LLMs are trained with large text datasets, including medical literature, and they can be leveraged to verify the discovered cause-effect hypothesis. However they can not verify hypotheses that have not been verified by the medical literature. ChatGPT agreed with most of the discovered causal hypotheses with positive effects, but it could not produce reliable citations. For causal hypotheses with negative effects, ChatGPT had to be instructed to reason about indirect effects to verify some of the discovered causal hypotheses.

Dataset. We use statistically de-identified medical claims data provided by a leading US-based health insurance company for repeat ER visit analysis. One advantage of insurance claims over electronic health records (EHR) is that they contain information from multiple healthcare providers. The dataset consists of 461,754 claims from the year 2015 to 2018 for 11,893 diabetic patients with at least one ER visit and one or more claims after the first ER visit. We observe from the dataset that nearly 80% of patients with multiple ER visits have a second ER visit within 12 months of the first one. The outcome Y is whether or not a patient visits the ER within 12 months of the first visit. The dataset consists of 45% patients with a repeat ER visit ($Y = 1$) within 12 months. We treat the ICD-10 diagnosis codes billed to patients as potential causes of the repeat ER visits. The data X correspond to 80% of most frequent ICD-10 codes and a binary out-of-vocabulary (OOV) indicator that captures the remaining less frequent ICD-10 codes among all diabetic populations. We flatten the claims of each patient using binary count aggregation that indicates the presence or absence of a diagnosis code. We ensure only the diagnosis codes encountered prior to measuring the outcome are aggregated. If $Y = 1$, the diagnosis codes before the second ER visit are aggregated, and if $Y = 0$, diagnosis codes up to 12 months after the first ER visit are aggregated.

For the hospital readmissions analysis, we use the freely available MIMIC-IV dataset [24] that is sourced from two in-hospital database systems, a custom hospital-wide EHR and an ICU-specific clinical information system. The dataset consists of de-identified data with diagnosis codes, admission records, and patient information from 2008 to 2019. For our study, we extract patient characteristics, hospitalization metadata, and the diagnosis codes with the ICD-9 version that gives 335,378 hospitalizations records for 173,034 patients. We consider 30 days as the time interval to check readmissions. The dataset consists of 17% patients with at least one readmission within 30 days of discharge ($Y = 1$). Similar to repeat ER visit analysis, we select potential causes as 70% most frequent diagnosis codes and an OOV indicator for the remaining less frequent codes. These codes are aggregated for each patient following the process similar to repeat ER visit analysis. For hospital readmission analysis, the data X includes patient characteristics such as age group, admission metadata such as previous discharge location, and diagnosis codes.

Results. For the real-world experiments, we consider three CSL algorithms in the ensemble module: HC [50], FGES [47], and MMHC [58]. The choice of the CSL algorithms is motivated by the high dimensionality of the variables and parallelized implementation of the algorithms. The output for MMHC and HC is a DAG and for FGES is a CPDAG (completed partially directed acyclic graph). We use temporal order of diagnosis codes as orientation support heuristic to orient a few undirected edges in the CPDAG. The Appendix provides details on orientation support heuristic, algorithm assumptions, and hyperparameters.

Figure 4 depicts the multi-set of average total causal effects (ATE) for top ICD-10 diagnosis codes on the repeat ER visits. Figure 4(a) shows top diagnosis codes with positive ATE that are indicators of risk factors for increased likelihood of repeat ER visits. Similarly, Figure 4(b) shows top diagnosis codes that are likely related to preventive

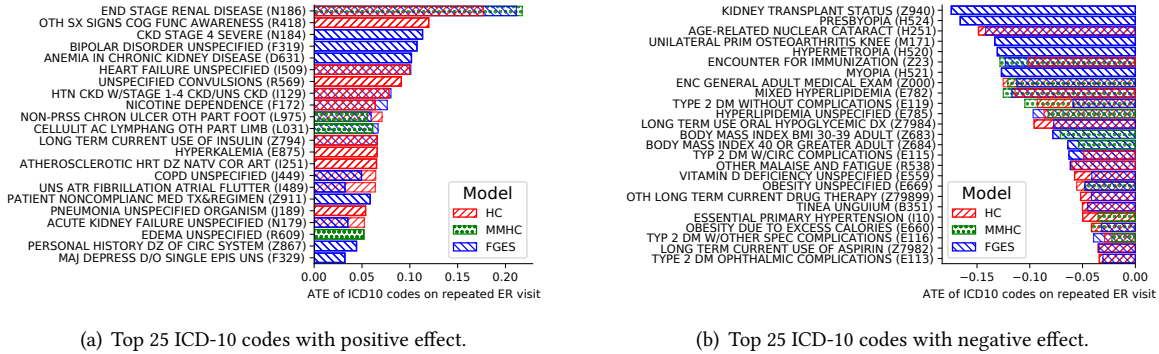


Fig. 4. Multi-set average total causal effect of top diagnosis codes on the repeat ER visits.

factors of repeat ER visits. Next, we summarize some interesting results produced by our approach and validate them using published research.

Patients with kidney, circulatory, respiratory, and mental health complications are vulnerable to repeat ER visits. This result is consistent to the model of risk factors for frequent ER visits validated by the Emergency Medicine physicians [6]. Kidney failure and dependence on dialysis are identified to be the causal factors for heavy ER utilization [27].

Interventions on patient noncompliance, insulin management, and smoking dependence can be further investigated to reduce repeat ER visits in diabetic population. Long-term use of insulin and patient noncompliance are discovered as risk factors for repeat ER visits consistent with previous studies [19, 26]. Nicotine dependence is likely a factor interacting with other causes because smoking is found to be associated with increased blood glucose levels and risk of cardiovascular and kidney comorbidities for diabetic patients [56].

Interventions encouraging regular checkups, immunization, and drug adherence can be investigated for reducing repeat ER visits. Figure 4(b) shows the ICD-10 codes with negative causal effects which can be considered as possible interventions or preventive factors. While some codes, such as Myopia, are not suitable as interventions, others, such as “Encounter of General Medical Exam (Z000)” and “Encounter for Immunization (Z23)” are. These preventive measures are recommended to diabetic population to prevent complications [7, 53]. The ICD-10 codes associated with long-term (current) use of drugs are likely proxies for drug adherence. *Potential interventions and heterogeneous causal effects.* Figure 5 depicts the ICD-10 diagnosis codes identified to produce heterogeneous causal effects for the two practical interventions, Z000 and Z23. The values in the x-axis are the differences of CATE of treatment X_j on repeat ER visits Y for patients with and without a diagnosis Z i.e. $X_{j,CATE}(Z = 1) - X_{j,CATE}(Z = 0)$. In Figure 5(a), we observe that intervention on the medical exam has less preventive effectiveness to patients with symptoms of convulsions (R569) compared to patients without convulsions. Figure 5 suggests interventions on both preventive measures for reducing repeat ER visits are less effective for diabetic patients with metabolic syndrome (primary hypertension (I10) or Hyperlipidemia (E785)) as well as for patients already utilizing health services such as drug use or dietary counseling.

Figure 6 depicts the multi-set of total causal effects for top ICD-9 diagnosis codes as well as other metadata on 30-day readmission. Figure 6(a) shows top diagnosis codes and other contexts with positive total causal effects indicative of risk factors. Figure 6(b) shows top diagnosis codes and contexts that are potential preventive factors of readmissions. Here, we outline some interesting results produced by our approach consistent with published research [5, 28].

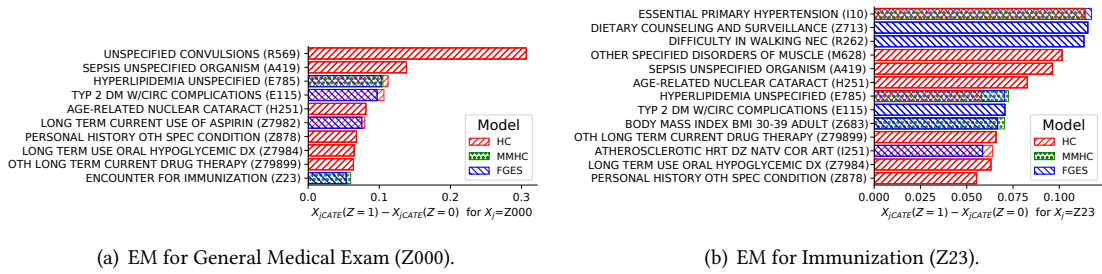


Fig. 5. Effect modifiers (EM) of two preventive diagnosis codes on repeat ER visits.

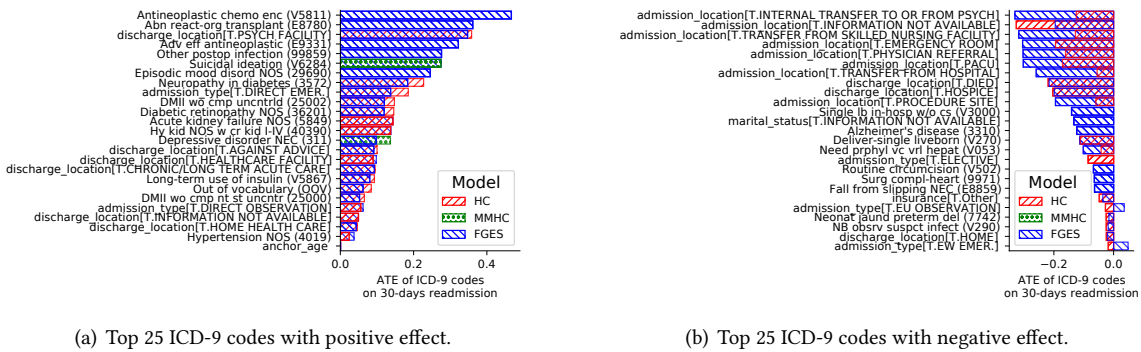


Fig. 6. Multi-set total causal effect for top diagnosis codes on 30-days readmissions identified by three CSL algorithms.

Surgical complications, adverse effects of drugs, and advanced chronic diseases are risk factors for readmissions. Figure 6(a) shows diagnosis codes related to surgical complications (E8780, 99859) and adverse effects of drugs (E9331) has significant ATE. Similarly, the codes linked to chronic conditions like diabetes (3572, 25002, 36201, V5867, 25000), kidney failure (5849, 40390), hypertension (4019, 40390), and cancer (V5811, E9331) are positive suggesting these subpopulations are vulnerable to readmissions.

Interventions targeting patients with mental health disorders should be investigated. In Figure 6(a), we notice the diagnosis codes related to suicidal ideation (V6284), episodic mood disorder (29690), and depressive disorder (311) have positive ATE.

Heterogeneity of readmissions based on admit and discharge locations should be further investigated for designing interventions. Figure 6(a) and 6(b) show various admit and discharge locations having diverse effects on readmissions. Patients admitted to the hospital directly (DIRECT EMER. and DIRECT OBSERVATION) are more likely to end up being readmitted within 30 days than patients admitted to other locations. Interestingly, patients discharged to psychiatric, healthcare, and chronic/long-term acute care facilities are more prone to readmissions. Patients discharged against advice have a higher readmission rate while discharged to hospice are discovered to be less likely for 30-days readmission. Additional investigation has to be done by the stakeholders to understand these behaviors.

Early diagnosis of risk factors can prevent readmissions. Figure 6(b) shows the quality of care such as the diagnosis of surgical cardiac complications (9971), observation for suspected infections (V290), and diagnosis of need for preventive vaccination (V053) reduces the likelihood of readmission.

7.2 Synthetic and Semi-synthetic Data Experiments

We perform synthetic and semi-synthetic experiments to evaluate the benefits of CSL ensemble over using a single algorithm. The experiments involve four steps: (1) generating ground-truth causal models, (2) generating (semi-)synthetic data from the models, (3) running experiments with the ensemble framework, and (4) evaluating the results.

Synthetic setup. We want to test how sensitive CSL algorithms are to structural properties like the number of nodes, the sparsity of edges, and the network topology in discovering the causes of a sink outcome node. Similar to Zheng et al. [65], we generate ground-truth directed acyclic graphs (DAGs) according to Erdős Rényi (*er*) [14] and Barabási Albert (*ba*) [1] random graph models by varying the number of nodes and connectivity parameters. The undirected degree distributions of *er* and *ba* graphs are binomial and power law due to random and preferential attachment edge adjacency, respectively. Both graphs are oriented with random topological order ensuring the outcome Y is never a parent. We defer the details to the Appendix.

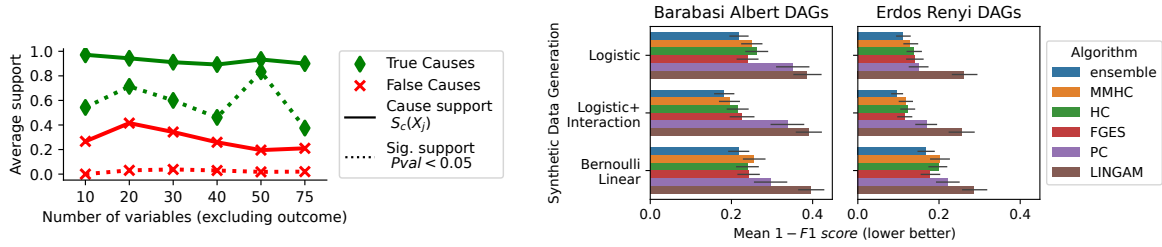
We consider three modes of synthetic data generation: *logistic*, *logistic+interaction*, and *Bernoulli linear*. The effect modification between variables due to non-linearity alone and due to both interaction and non-linearity are respectively captured by the *logistic* and *logistic+interaction* data generations. There is no effect modification in the *Bernoulli linear* data generation, and the size of the causal effects may be small. Appendix presents the detailed functional forms.

Semi-synthetic setup. In addition to randomly generated graphs, we use real-world data to generate ground truth causal graphs and learn their SCM parameters. We use a base algorithm to learn a causal graph and its parameters which we consider as the ground truth. We present analysis with MMHC as base algorithm but we get similar trends for other base algorithms. Top $N \in \{10, 20, 30, 40, 50, 75\}$ most frequent diagnosis codes along with the outcome are selected from the aggregated data, described in §7.1, for generating ground-truth graphs of different sizes. The top N codes include an out-of-vocabulary (OOV) variable indicating presence of other less frequent diagnosis codes. This data is used to learn a ground-truth causal model $G_T(V_T, E_T)$. If any edges in the causal model are unoriented, we use orientation support, defined in the Appendix, to orient these edges. From the ground-truth causal graph, we estimate the SCM parameters as conditional probability tables (CPT) $p(V_i|pa(V_i, G_T))$. Using the CPT and the topological ordering of the ground truth causal DAG, we sample IID semi-synthetic data.

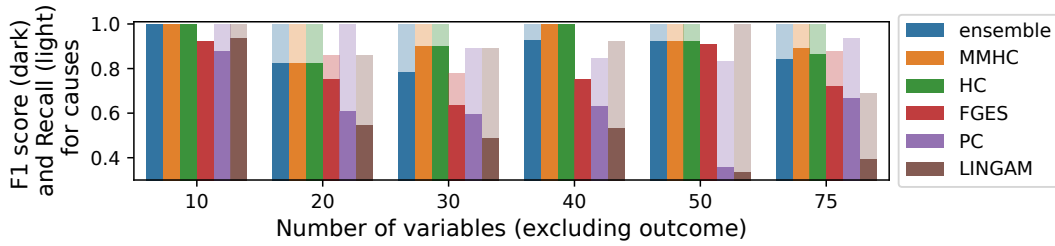
Results. Next, we present main takeaways from the evaluation of the experiments with an ensemble of MMHC, HC, FGES, PC, and LINGAM [52] algorithms.

The ensemble approach can rank potential causal hypotheses. Figure 7(a) shows the CSL algorithms in an ensemble, for semi-synthetic data, have more than 90% average agreement (i.e., cause support) for true causes whereas the average agreement for false causes is far less. This indicates that CSL algorithms, despite diverse approaches and assumptions, tend to agree more on true causes than on false causes. Similarly, as seen in Figure 7(a), the estimated total effects for false-positive causes is mostly statistically insignificant ($p \geq 0.05$). Synthetic experiments included in Appendix yield a similar result. Therefore, the cause support metric, the magnitude of the total effects, and confident scores with p-value obtained from the ensemble help to rank the causal hypotheses.

A simple majority voting ensemble to determine the causes offers robustness to data generation mechanisms, network topology, number of nodes, and density of edges. The performance of a majority voting ensemble and individual algorithms for identifying causes of Y is summarized in Figure 7(b) in terms of the $(1 - F1 \text{ score})$ metric for three synthetic data generation mechanisms and two DAG generation mechanisms. For each DAG type and data generation type, compared to any individual algorithm, the ensemble approach has the best performance in average across DAGs with different number of nodes and density of edges. The results show that the ensemble provides increased robustness than committing to a single algorithm. Appendix explains the detailed experimental setup and additional results consistent with the above observation.



(a) CSL algorithms in an ensemble have higher average agree- (b) A majority voting ensemble and individual algorithms for different data ment on true causes. generation, graph topology, and edge density in terms of 1-F1 score.



(c) A majority voting ensemble and individual algorithms in terms of recall and F1 scores.

Fig. 7. Evaluation of the ensemble approach with synthetic (b) and semi-synthetic (a and c) data.

A simple majority voting ensemble to determine the causes favors high recall while maintaining fair precision. Figure 7(c) shows the performance of individual algorithms and ensemble in terms of recall and F1 scores for the semi-synthetic data generation. We notice, as expected, MMHC and HC with similar methodology or assumptions with the underlying data generation process have good performances while other algorithms with different assumptions and methodologies have slightly poorer performances. LINGAM with incompatible assumptions has a lower F1 score. The ensemble is able to maintain a high recall with decent F1 score. We note that majority voting may perform poorly when the performance of each base algorithm is poor, for example, due to limited sample size. Therefore, we prefer ranking the causes utilizing confidence measures as demonstrated with real-world results. The results of synthetic and semi-synthetic experiments show that the ensemble approach is robust in discovering potential causes with a measure of confidence.

8 Conclusion

In this paper, we investigate the problem of discovering causes and effect modifiers of an outcome using observational data. We focus on practical scenarios where there is uncertainty in cause-and-effect hypotheses generated by CSL algorithms. We propose a framework that incorporates an ensemble of CSL algorithms, effect modifiers discovery, and heterogeneous effect estimation to output causes and effect modifiers of the outcome consistent across multiple causal models. Using synthetic and semi-synthetic experiments, we show the benefits of using an ensemble of CSL algorithms for discovery tasks. We demonstrate the promise of our approach with real-world use cases of discovering causes and sources of heterogeneity of repeat ER visits for diabetic patients and hospital readmission for ICU patients. The evaluation of the results utilizing published research literature shows our framework automatically generates causal hypotheses consistent with known knowledge.

References

[1] Réka Albert and Albert-László Barabási. 2002. Statistical mechanics of complex networks. *Reviews of modern physics* 74, 1 (2002), 47.

- [2] Susan Athey and Guido Imbens. 2016. Recursive partitioning for heterogeneous causal effects. *Proceedings of the National Academy of Sciences* 113, 27 (2016), 7353–7360.
- [3] Molly K Bailey, Audrey J Weiss, Marguerite L Barrett, and H Joanna Jiang. 2019. Characteristics of 30-Day All-Cause Hospital Readmissions, 2010–2016: Statistical Brief# 248. *Healthcare Cost and Utilization Project (HCUP) Statistical Briefs* (2019).
- [4] Laurence C Baker and Linda Schuurman Baker. 1994. Excess cost of emergency department visits for nonurgent care. *Health affairs* 13, 5 (1994), 162–171.
- [5] Ivy Benjenk and Jie Chen. 2018. Effective mental health interventions to reduce hospital readmission rates: a systematic review. *JHMHP* 2 (2018).
- [6] Lauren E Birmingham, Vinay K Cheruvu, Jennifer A Frey, Kirk A Stiffler, and Jonathan VanGeest. 2020. Distinct subgroups of emergency department frequent users: a latent class analysis. *Emergency Medicine* 38, 1 (2020), 83–88.
- [7] CDC. 2021. Your Diabetes Care Schedule. <https://www.cdc.gov/diabetes/managing/care-schedule.html>. Accessed: 2021-09-05.
- [8] David Chickering. 2002. Optimal structure identification with greedy search. *JMLR* 3, Nov (2002), 507–554.
- [9] David Maxwell Chickering. 1995. A transformational characterization of equivalent Bayesian network structures. In *UAI*. 87–98.
- [10] CMS. 2021. Hospital Readmissions Reduction Program. <https://www.cms.gov/medicare/medicare-fee-for-service-payment/acuteinpatientpps/readmissions-reduction-program>. Accessed: 2022-02-06.
- [11] Diego Colombo and Marloes H Maathuis. 2014. Order-Independent Constraint-Based Causal Structure Learning. *JMLR* 15, 116 (2014), 3921–3962.
- [12] Tim Cooksley, Hanneke Merten, John Kellett, Mikkel Brabrand, Rachel Kidney, C Nickel, Prabath WB Nanayakkara, and Chris P Subbe. 2015. PRISMA analysis of 30 day readmissions to a tertiary cancer hospital. *Acute Med* 14, 2 (2015), 53–56.
- [13] Babiche EJM Driesen, Hanneke Merten, Cordula Wagner, H Jaap Bonjer, and Prabath WB Nanayakkara. 2020. Unplanned return presentations of older patients to the emergency department: a root cause analysis. *BMC geriatrics* 20, 1 (2020).
- [14] Paul Erdős, Alfréd Rényi, et al. 1960. On the evolution of random graphs. *Publ. Math. Inst. Hung. Acad. Sci* 5, 1 (1960), 17–60.
- [15] Amanda Gentzel, Dan Garant, and David Jensen. 2019. The case for evaluating causal models using interventional measures and empirical data. *NIPS* 32 (2019).
- [16] Maria Glans, Annika Kragh Ekstam, Ulf Jakobsson, Åsa Bondesson, and Patrik Midlöv. 2020. Risk factors for hospital readmission in older adults within 30 days of discharge—a comparative retrospective study. *BMC geriatrics* 20, 1 (2020).
- [17] Clark Glymour, Kun Zhang, and Peter Spirtes. 2019. Review of causal discovery methods based on graphical models. *Frontiers in Genetics* 10 (2019).
- [18] Chang Gong, Di Yao, Chuzhe Zhang, Wenbin Li, and Jingping Bi. 2023. Causal Discovery from Temporal Data: An Overview and New Perspectives. *arXiv preprint arXiv:2303.10112* (2023).
- [19] Caleb W Grote and Douglas E Wright. 2016. A role for insulin in diabetic neuropathy. *Frontiers in neuroscience* 10 (2016), 581.
- [20] David Heckerman, Dan Geiger, and David M Chickering. 1995. Learning Bayesian networks: The combination of knowledge and statistical data. *Machine learning* 20, 3 (1995), 197–243.
- [21] Christina Heinze-Deml, Marloes H Maathuis, and Nicolai Meinshausen. 2018. Causal structure learning. *Annual Review of Stats. and its App.* 5 (2018), 371–391.
- [22] Hengyi Hu and Larry Kerschberg. 2023. Improving Causal Bayesian Networks using Expertise in Authoritative Medical Ontologies. *ACM Transactions on Computing for Healthcare* 4, 4 (2023), 1–32.
- [23] Catherine Hudon, Josiane Courteau, Cynthia Krieg, and Alain Vanasse. 2017. Factors associated with chronic frequent emergency department utilization in a population with diabetes living in metropolitan areas: a population-based retrospective cohort study. *BMC health services research* 17, 1 (2017), 1–9.
- [24] Alistair Johnson, Lucas Bulgarelli, Tom Pollard, Steven Horng, Leo Anthony Celi, and R Mark IV. 2021. MIMIC-IV (version 1.0). *PhysioNet* (2021).
- [25] Marcus Kaiser and Maksim Sipos. 2022. Unsuitability of NOTEARS for Causal Graph Discovery when Dealing with Dimensional Quantities. *Neural Processing Letters* (2022), 1–9.
- [26] Abbas E Kitabchi, Guillermo E Umpierrez, John M Miles, and Joseph N Fisher. 2009. Hyperglycemic crises in adult patients with diabetes. *Diabetes care* 32, 7 (2009), 1335–1343.
- [27] Paul Komenda, Navdeep Tangri, Evan Klajnjar, Amanda Eng, Michelle Di Nella, Brett Hiebert, Trevor Strome, Ricardo Lobato de Faria, James M Zacharias, Mauro Verrelli, et al. 2018. Patterns of emergency department utilization by patients on chronic dialysis: A population-based study. *PLoS ONE* 13, 4 (2018).
- [28] Sunil Kripalani, Cecelia N Theobald, Beth Ancil, and Eduard E Vasilevskis. 2014. Reducing hospital readmission rates: current strategies and future directions. *Annual review of medicine* 65 (2014), 471–485.
- [29] Sören R Künzel, Jasjeet S Sekhon, Peter J Bickel, and Bin Yu. 2019. Metalearners for estimating heterogeneous treatment effects using machine learning. *Proceedings of the National Academy of Sciences* 116, 10 (2019), 4156–4165.
- [30] Aaron L Leppin, Michael R Gionfriddo, Maya Kessler, Juan Pablo Brito, Frances S Mair, Katie Gallacher, Zhen Wang, Patricia J Erwin, Tanya Sylvester, Kasey Boehmer, et al. 2014. Preventing 30-day hospital readmissions: a systematic review and meta-analysis of

- randomized trials. *JAMA* 174, 7 (2014), 1095–1107.
- [31] Marloes H Maathuis, Markus Kalisch, and Peter Bühlmann. 2009. Estimating high-dimensional intervention effects from observational data. *The Annals of Statistics* 37, 6A (2009), 3133–3164.
- [32] Ruth E Malone. 1998. Whither the almshouse? Overutilization and the role of the emergency department. *JHPPL* 23, 5 (1998), 795–832.
- [33] Christopher Meek. 1995. Causal inference and causal explanation with background knowledge. In *UAI*. 403–410.
- [34] National Institute of Justice. 2021. Recidivism. <https://nij.ojp.gov/topics/corrections/recidivism>. Accessed: 2021-08-10.
- [35] New England Health Institute. 2010. A Matter of Urgency: Reducing Emergency Department Overuse, A NEHI Research Brief – March 2010. https://www.nehi.net/writable/publication_files/file/neh_i_ed_overuse_issue_brief_032610final.pdf. Accessed: 2021-06-05.
- [36] Atefeh Noori, Mostafa Shokoohi, Mohammad Reza Baneshi, Nasim Naderi, Hooman Bakhshandeh, and Ali Akbar Haghdoost. 2014. Impact of socio-economic status on the hospital readmission of Congestive Heart Failure patients: a prospective cohort study. *Journal of health policy and management* 3, 5 (2014), 251.
- [37] Galia Nordon, Gideon Koren, Varda Shalev, Benny Kimelfeld, Uri Shalit, and Kira Radinsky. 2019. Building causal graphs from medical literature and electronic medical records. In *Proceedings of the AAAI Conference on Artificial Intelligence*, Vol. 33. 1102–1109.
- [38] Juan Miguel Ogarrio, Peter Spirtes, and Joe Ramsey. 2016. A hybrid causal search algorithm for latent variable models. In *Conference on Probabilistic Graphical Models*. 368–379.
- [39] Judea Pearl. 1988. *Probabilistic Reasoning in Intelligent Systems: Networks of Plausible Inference*. Morgan Kaufmann.
- [40] Judea Pearl. 2009. *Causality*. Cambridge university press.
- [41] Judea Pearl. 2015. Detecting Latent Heterogeneity. *Sociological Methods & Research* 1 (2015), 20.
- [42] Lauren S Penney, Musarrat Nahid, Luci K Leykum, Holly Jordan Lanham, Polly H Noël, Erin P Finley, and Jacqueline Pugh. 2018. Interventions to reduce readmissions: can complex adaptive system theory explain the heterogeneity in effectiveness? A systematic review. *BMC health services* 18, 1 (2018), 1–10.
- [43] Emilija Perkovic, Markus Kalisch, and Marloes H Maathuis. 2017. Interpreting and using CPDAGs with background knowledge. In *UAI*. AUAI Press, ID–120.
- [44] Emilija Perkovic, Johannes Textor, Markus Kalisch, and Marloes H Maathuis. 2017. Complete graphical characterization and construction of adjustment sets in Markov equivalence classes of ancestral graphs. *JMLR* 18, 1 (2017), 8132–8193.
- [45] Jonas Peters, Dominik Janzing, and Bernhard Schölkopf. 2011. Causal inference on discrete data using additive noise models. *IEEE Transactions on Pattern Analysis and Machine Intelligence* 33, 12 (2011), 2436–2450.
- [46] Patient Protection and Affordable Care Act. 2019. Hospital readmissions reduction program. Pub L No. 111–148, 124 Stat 408, S3025.
- [47] Joseph Ramsey, Madelyn Glymour, Ruben Sanchez-Romero, and Clark Glymour. 2017. A million variables and more: the Fast Greedy Equivalence Search algorithm for learning high-dimensional graphical causal models, with an application to functional magnetic resonance images. *IJDSA* 3, 2 (2017), 121–129.
- [48] Michael A Ross, Robin R Hemphill, Jerome Abramson, Kim Schwab, and Carol Clark. 2010. The recidivism characteristics of an emergency department observation unit. *Annals of emergency medicine* 56, 1 (2010), 34–41.
- [49] RJ Salway, R Valenzuela, JM Shoenberger, WK Mallon, and A Viccellio. 2017. Emergency department (ED) overcrowding: evidence-based answers to frequently asked questions. *Revista Médica Clínica Las Condes* 28, 2 (2017), 213–219.
- [50] Marco Scutari. 2010. Learning Bayesian Networks with the bnlearn R Package. *JSS* 35, 3 (2010), 1–22. doi:10.18637/jss.v035.i03
- [51] Sophia Sheikh. 2019. Risk factors associated with emergency department recidivism in the older adult. *Western Jour. of Emer. Med.* 20, 6 (2019), 931.
- [52] Shohei Shimizu, Patrik O Hoyer, Aapo Hyvärinen, Antti Kerminen, and Michael Jordan. 2006. A linear non-Gaussian acyclic model for causal discovery. *JMLR* 7, 10 (2006).
- [53] Steven A Smith and Gregory A Poland. 2000. Use of influenza and pneumococcal vaccines in people with diabetes. *Clinical Diabetology* 1, 1 (2000), 13–32.
- [54] Lesley JJ Soril, Laura E Leggett, Diane L Lorenzetti, Tom W Noseworthy, and Fiona M Clement. 2015. Reducing frequent visits to the emergency department: a systematic review of interventions. *PloS one* 10, 4 (2015), e0123660.
- [55] Peter Spirtes, Clark N Glymour, Richard Scheines, and David Heckerman. 2000. *Causation, prediction, and search*. MIT press.
- [56] Serena Tonstad. 2009. Cigarette smoking, smoking cessation, and diabetes. *Diabetes research and clinical practice* 85, 1 (2009), 4–13.
- [57] Stephen Trzeciak and Emanuel P Rivers. 2003. Emergency department overcrowding in the United States: an emerging threat to patient safety and public health. *Emergency medicine journal* 20, 5 (2003), 402–405.
- [58] Ioannis Tsamardinos, Laura E Brown, and Constantin F Aliferis. 2006. The max-min hill-climbing Bayesian network structure learning algorithm. *Machine Learning* 65, 1 (2006), 31–78.
- [59] W Van Vuuren, CE Shea, Tjerk W Van Der Schaaf, and Pays-Bas). Technische hogeschool (Eindhoven. 1997. *The development of an incident analysis tool for the medical field*. Eindhoven University of Technology, Eindhoven.
- [60] Tyler VanderWeele and James Robins. 2007. Four types of effect modification: a classification based on directed acyclic graphs. *Epidemiology* 18, 5 (2007), 561–568.

- [61] Lidón Villanueva, Selene Valero-Moreno, Keren Cuervo, and Vicente J Prado-Gascó. 2019. Sociodemographic variables, risk factors, and protective factors contributing to youth recidivism. *Psicothema* 31, 2 (2019), 128–133.
- [62] Wei Wang, Gangqiang Hu, Bo Yuan, Shandong Ye, Chao Chen, Yayun Cui, Xi Zhang, and Liting Qian. 2020. Prior-Knowledge-Driven Local Causal Structure Learning and Its Application on Causal Discovery Between Type 2 Diabetes and Bone Mineral Density. *IEEE Access* 8 (2020), 108798–108810.
- [63] Chirayu Wongchokprasitti, Harry Hochheiser, Jeremy Espino, Eamonn Maguire, Bryan Andrews, Michael Davis, and Chris Inskip. 2019. `bd2kccd/py-causal`.
- [64] Xun Zheng, Bryon Aragam, Pradeep K Ravikumar, and Eric P Xing. 2018. Dags with no tears: Continuous optimization for structure learning. *Advances in Neural Information Processing Systems* 31 (2018).
- [65] Xun Zheng, Chen Dan, Bryon Aragam, Pradeep Ravikumar, and Eric Xing. 2020. Learning sparse nonparametric dags. In *International Conference on Artificial Intelligence and Statistics*. PMLR, 3414–3425.

Appendix

Here we provide the following supplementary materials for the main paper:

- (1) Description of causal structure learning algorithms,
- (2) Description and results of simulated data experiments,
- (3) Details, including pseudocode, for orienting undirected edges of a DAG's equivalence class,
- (4) Additional details of the experimental setup and hyperparameters.

Causal Structure Learning (CSL) and Algorithms

The idea for CSL is to utilize conditional independencies (CI) in the data distribution to infer the structure of the causal graphical model. The joint distribution P described by $G(\mathbf{V}, \mathbf{E})$ factorizes to the product of the conditional probability of each random variable given its parents according to causal Markov assumption, i.e., $P(V_1, \dots, V_n) = \prod_{i=1}^n P(V_i | pa(V_i, G))$. The notion of *d-separation* [39, 40] is used to read off all CI that hold for any data distribution that is generated by the mechanism described by a graphical model. The same conditional independence relation can be satisfied by multiple causal models belonging to a Markov equivalence class, and CSL generally concerns learning a Markov equivalence class. Additional parametric assumptions and background knowledge are needed to identify a causal model within the equivalence class. We summarize four categories of causal structure learning algorithms according to their approach: (1) constraint-based, (2) scored-based, (3) hybrid, and (4) functional causal model-based.

Constraint-Based algorithms, such as PC [11, 55] and Fast Causal Inference (FCI) [55], use conditional independencies in the data as constraints to estimate an equivalence class of underlying SCM. The PC algorithm makes assumptions of causal sufficiency and faithfulness for the correctness of edge adjacencies. Then, v-structure discovery followed by Meek orientation rules [33] produces an equivalence class graph, also known as a completed partial directed acyclic graph (CPDAG). FCI is also a constraint-based algorithm that relaxes the causal sufficiency assumption of PC algorithm. FCI outputs a partial ancestral graph (PAG), a Markov equivalence class of maximal ancestral graph (MAG), to incorporate the hidden confounders using a bidirectional arrow, i.e., $V_i \leftrightarrow V_j$. In a PAG, $V_i \rightarrow V_j$ is interpreted as V_i being an ancestor of V_j and V_j not being an ancestor of V_i . Similarly, $V_i \circ \rightarrow V_j$ indicates either V_i is an ancestor of V_j and/or there is a hidden confounder between V_i and V_j , but V_j is not an ancestor of V_i .

Score-based algorithms, such as Greedy Equivalence Search (GES) [8] and Fast GES [47], consider causal structure learning as the problem of fitting a CPDAG to the data according to a relevant score function that relates to how well the CPDAG captures the conditional independencies in the data. FGES's implementation in `py-causal` [63] package provides some robustness to faithfulness assumption. These algorithms assume causal sufficiency. Under the fulfilment of assumptions and infinite sample size with absence of selection bias, both PC and GES algorithms are shown to be sound and complete.

Hybrid algorithms combine both constraint-based and score-based approaches. Max-Min Hill Climbing (MMHC) [58] uses a constraint-based Max-Min Parents and Children (MMPC) local discovery algorithm for skeleton determination and a score-based Hill-Climbing (HC) [50] for edges orientation. GFCE [38] is a hybrid algorithm that relaxes causal sufficiency assumption.

The functional causal models [17] use SCM with additional assumptions on the distribution of \mathbf{U} and \mathbf{V} to distinguish between different DAGs in the same equivalence class. Linear Non-Gaussian Acyclic Model (LINGAM) [52] assumes causal sufficiency, linear data generating process, and exogeneous variables with Non-Gaussian distributions of non-zero variance. Although, additive noise model for discrete data have been proposed, it is too restrictive for binary variables [45]. Recently, methods using continuous optimization [64, 65] are popular

for extracting a DAG structure from observational data. However, these methods performed poorly on our synthetic data and we excluded them from our analysis.

Simulated Experiments

Here, we provide additional details on simulated experiments including random graph and data generation as well as experimental results supporting the results presented in the main paper. A simulated experimental setup is necessary for the evaluation of causal discovery methods because there is a lack of ground truth in real-world datasets. Synthetic data provides flexibility to test our hypothesis. However, using purely synthetic data for evaluating causal models may have limitations like high “researcher degrees-of-freedom” and lack of standardization [15]. A semi-synthetic data generation strategy, that utilizes features of real-world data, helps in mitigating some of these limitations. Therefore, we employ both synthetic and semi-synthetic data generation methods to evaluate the benefits of our causal structural learning ensemble over using a single CSL algorithm. Synthetic data generation representing the phenomena of repeated undesirable outcomes is non-trivial. Instead, we focus on simulated experiments with IID data obtained with Bag-of-Events (BOE) representation.

Ground truth causal graph generation

Synthetic. We want to test how sensitive CSL algorithms are to structural properties like the number of nodes, the sparsity of edges, and the network topology in discovering the causes of a sink outcome node. For this reason, we generate ground-truth directed acyclic graphs (DAGs) according to Erdos-Renyi (ER) and Barabasi-Albert (BA) random graph models by varying the number of nodes (n) and connectivity parameters. The undirected ER graph is controlled by the edge probability parameter p , while the BA graph is controlled by the preferential attachment parameter m , referred to as the sparsity parameter (sp_{ba}). For consistency, we define the sparsity parameter $sp_{er} | p = \frac{2 \times n \times sp_{er}}{n \times (n-1)}$ for the ER graph as well indicating average degree of graph.

Next, we orient the undirected edges of the generated ER and BA graphs according to a random topological order of nodes. We also add a sink outcome node to the oriented graph. For the ER graph, k nodes are connected to the outcome node such that the average degree sp_{er} is maintained. For the BA graph, we calculate the uniform edge probability for the existing graph and then randomly connect existing nodes to the outcome node according to the edge probability. This process gives us random DAGs with a sink outcome node.

Semi-Synthetic. In addition to randomly generated graphs, we use real-world data to generate ground truth causal graphs and learn their SCM parameters. We use a base algorithm to learn a causal graph and its parameters which we consider as the ground truth. We present analysis with MMHC as base algorithm but we get similar trends for other base algorithms. The causal model is learned from the real-world insurance claims data. The data is preprocessed with $\tau = 12$ months as time interval for repeated undesirable outcome. Top $N \in \{10, 20, 30, 40, 50, 75\}$ most frequent events along with the outcome are subset from the aggregated Bag-of-events (BOE) data representation based on frequency of diagnosis codes for generating ground-truth graphs of different sizes. The top N include an out-of-vocabulary (OOV) variable indicating presence of other less frequent events. This data is used to learn a causal model $G_T(\mathbf{V}_T, \mathbf{E}_T)$. If any edges in the causal model are unoriented, we use orientation support, defined in the next section, to orient these edges.

Data generation

Synthetic. We consider three modes of data generation for synthetic experiments, focusing on binary data, with the following functional form:

- (1) *Logistic (L)*. $X = \text{Bernoulli}(\text{sigmoid}(b + \mathbf{W} \times pa(X, G)))$, where G is ground truth graph, $b \in \mathbb{R}$, and $\mathbf{W} \in \mathbb{R}^L$ with $L = \text{cardinality}(pa(X, G))$.
- (2) *Logistic + Interaction (LL)*. $X = \text{Bernoulli}(\text{sigmoid}(b + \mathbf{W} \times pa(X, G) + \mathbf{I} \times \text{combination}(pa(X, G), 2)))$, where $\mathbf{I} \in \mathbb{R}^{\binom{L}{2}}$, $b \in \mathbb{R}$, and $\mathbf{W} \in \mathbb{R}^L$.
- (3) *Bernoulli Linear (BL)*. $X = \text{Bernoulli}(b + \mathbf{W} \times pa(X, G))$, where $b \in (0, 1)$, $\mathbf{W} \in (-1, 1)^L$, and $0 \leq b + \mathbf{W} \times pa(X, G) \leq 1$.

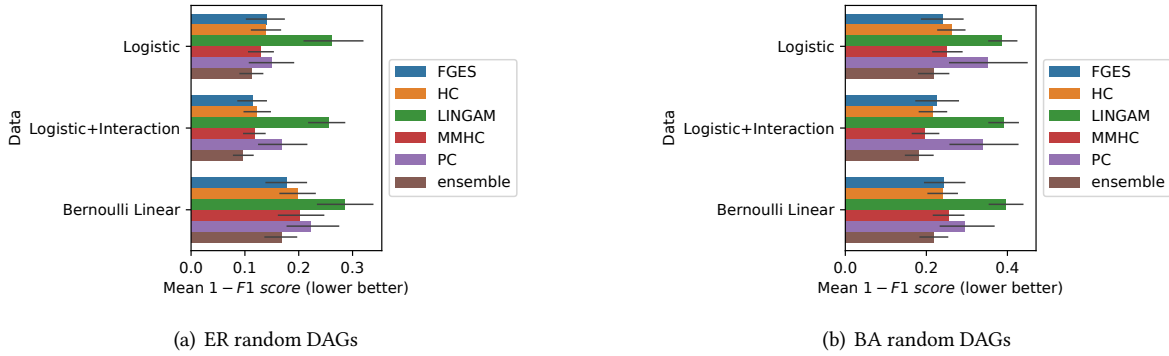


Fig. 8. Summarizing Tables 7 to 12: Performance of individual algorithms and ensemble in terms of mean 1-F1 score (lower better). Ensemble reduces the sensitivity to variation in structural properties like the number of nodes, the sparsity of edges, and network topology. An ensemble provides robustness compared to selecting a single algorithm.

Semi-Synthetic. From the ground-truth causal graph, we estimate the SCM parameters as conditional probability tables (CPT) $p(V_i | pa(V_i, G_T))$. Using the SCM parameters and the topological ordering of the ground truth causal DAG, we sample synthetic data in the BOE representation.

Evaluation metrics

To assess the performance of the ensemble approach in refining potential causal factors, we estimate the average causal support for the true causes ($TP(S_c)$) and the false causes ($FP(S_c)$) defined as $TP(S_c) = \frac{\sum_{X^j \in anc(Y, G_T)} S_c(X^j)}{n(anc(Y, G_T))}$, and $FP(S_c) = \frac{\sum_{X^j \notin anc(Y, G_T)} S_c(X^j)}{n(G_T) - n(anc(Y, G_T))}$, where Y is the outcome and $S_c(X^j)$ is the cause support for event X^j . The $TP(S_c)$ and $FP(S_c)$ measures indicate the agreement among multiple CSL algorithms for true causes and false causes, respectively. In addition to the structural cause support, we investigate significance support by checking the fraction of algorithms with statistically significant ($pvalue < 0.05$) total effects for the identified causes. The significance support gives a measure of confidence for discovered causes. Moreover, we compare individual algorithms and the ensemble in terms of precision, recall, and F1 scores of discovering true causes.

Simulated experiment results

The main paper presented results from the semi-synthetic experimental setup. Here, we describe the evaluation results for the following synthetic experimental setups.

Sensitivity to structural properties like the number of nodes, the sparsity of edges, and the network topology. In this setup, we randomly generate DAGs with ER and BA topologies by varying nodes (excluding sink outcome) $n \in \{10, 20, 30, 40\}$ as well as sparsity parameters $sp_{er} \in \{0.8, 1.0, 1.5, 2.0\}$ and $sp_{ba} \in \{1, 2, 3, 4\}$. For each combination of the number of nodes and sparsity parameters, we generate 5 random DAGs. Then, we generate data according to logistic (L), logistic + interaction (LL), and Bernoulli linear (BL) functional forms 3 times each with different parameters for each DAG. We run an ensemble of five CSL algorithms: PC, FGES, HC, MMHC, and LINGAM. The assumptions of first four algorithms are similar but they differ in their methodology and hyperparameters (describe later). LINGAM, although incompatible with binary data, is included to test the robustness of ensemble toward noisy base learner. PC and FGES may return CPDAGs while MMHC, HC, and LINGAM return DAGs. We run bootstrapped version of MMHC and HC algorithms for 20 runs and leave edges undirected if they support each orientation 50% of the time. The evaluation results consider an $anc(Y, G_{est})$ query

that returns all ancestors with a directed path to the outcome node Y , ignoring undirected edges in the estimated graph.

Tables 1 to 6 show the average causal support (agreement) of the ensemble for true causes and false causes of the sink outcome node. These results are consistent with Figure 6 in the main paper, where the algorithms in the ensemble have higher agreement (support) on true causes and lower support for false causes. The significance support shows that it can be used to rank the causes for higher precision.

Tables 7 to 12 show the performance of the ensemble compared to each algorithm in terms of F1 score for different settings of structural parameters. It is observed that the performance of algorithms varies according to the structural properties and the ground truth structure, although most of the assumptions are satisfied and the sample size is decent ($n \times 1000$). It is revealed that the ensemble has the least deviation from the maximum F1 score. Figure 2 summarizes Tables 7 to 12, showing the ensemble has the best performance on average compared to the individual base algorithms. This indicates an ensemble provides robustness compared to selecting a single algorithm for practical settings with uncertain ground-truth structural properties. We notice the CSL algorithms have relatively better performance for ER model compared to BA model with preferential attachment mechanism. In both topologies, the ensemble improves the performance on average.

Nodes	10				20				30				40			
Sparsity	0.8	1.0	1.5	2.0	0.8	1.0	1.5	2.0	0.8	1.0	1.5	2.0	0.8	1.0	1.5	2.0
Support																
True Causes	0.88	0.81	0.84	0.86	0.83	0.91	0.78	0.81	0.93	0.78	0.78	0.86	0.94	0.84	0.90	0.80
True Causes (sig)	0.88	0.76	0.79	0.81	0.80	0.90	0.72	0.76	0.86	0.73	0.73	0.74	0.94	0.82	0.83	0.68
False Causes	0.05	0.09	0.17	0.09	0.03	0.04	0.16	0.27	0.03	0.06	0.15	0.17	0.02	0.07	0.09	0.19
False Causes (sig)	0.04	0.07	0.11	0.05	0.02	0.02	0.08	0.17	0.02	0.05	0.06	0.08	0.01	0.03	0.02	0.07

Table 1. Average cause support scores by an ensemble for True and False causes of a sink outcome node for random Erdos-Renyi DAGs with logistic data.

Nodes	10				20				30				40			
Sparsity	0.8	1.0	1.5	2.0	0.8	1.0	1.5	2.0	0.8	1.0	1.5	2.0	0.8	1.0	1.5	2.0
Support																
True Causes	0.86	0.85	0.81	0.85	0.82	0.89	0.76	0.83	0.92	0.77	0.80	0.86	0.94	0.83	0.89	0.81
True Causes (sig)	0.86	0.72	0.76	0.79	0.78	0.88	0.70	0.76	0.81	0.71	0.75	0.72	0.93	0.79	0.80	0.69
False Causes	0.06	0.09	0.20	0.03	0.03	0.04	0.13	0.24	0.04	0.07	0.11	0.15	0.02	0.06	0.06	0.17
False Causes (sig)	0.04	0.06	0.13	0.00	0.02	0.01	0.08	0.14	0.02	0.04	0.05	0.07	0.01	0.03	0.02	0.05

Table 2. Average cause support scores by an ensemble for True and False causes of a sink outcome node for random Erdos-Renyi DAGs with logistic+interaction data.

Nodes	10				20				30				40			
Sparsity	0.8	1.0	1.5	2.0	0.8	1.0	1.5	2.0	0.8	1.0	1.5	2.0	0.8	1.0	1.5	2.0
Support																
True Causes	0.88	0.81	0.84	0.86	0.83	0.91	0.78	0.81	0.93	0.78	0.78	0.86	0.94	0.84	0.90	0.80
True Causes (sig)	0.88	0.76	0.79	0.81	0.80	0.90	0.72	0.76	0.86	0.73	0.73	0.74	0.94	0.82	0.83	0.68
False Causes	0.05	0.09	0.17	0.09	0.03	0.04	0.16	0.27	0.03	0.06	0.15	0.17	0.02	0.07	0.09	0.19
False Causes (sig)	0.04	0.07	0.11	0.05	0.02	0.02	0.08	0.17	0.02	0.05	0.06	0.08	0.01	0.03	0.02	0.07

Table 3. Average cause support scores by an ensemble for True and False causes of a sink outcome node for random Erdos-Renyi DAGs with logistic data.

Nodes	10				20				30				40			
Sparsity	1	2	3	4	1	2	3	4	1	2	3	4	1	2	3	4
Support																
True Causes	0.79	0.82	0.64	0.66	0.79	0.79	0.65	0.74	0.89	0.84	0.74	0.78	0.85	0.79	0.77	0.63
True Causes (sig)	0.70	0.77	0.55	0.54	0.77	0.69	0.45	0.65	0.89	0.77	0.59	0.67	0.81	0.71	0.70	0.44
False Causes	0.13	0.36	0.18	0.27	0.05	0.27	0.35	0.40	0.05	0.20	0.37	0.39	0.06	0.16	0.25	0.46
False Causes (sig)	0.04	0.20	0.11	0.10	0.02	0.08	0.11	0.22	0.01	0.08	0.15	0.15	0.01	0.05	0.11	0.22

Table 4. Average cause support scores by an ensemble for True and False causes of a sink outcome node for random Barabasi-Albert DAGs with logistic data.

Nodes	10				20				30				40			
Sparsity	1	2	3	4	1	2	3	4	1	2	3	4	1	2	3	4
Support																
True Causes	0.78	0.77	0.70	0.70	0.82	0.70	0.72	0.73	0.91	0.87	0.72	0.78	0.85	0.79	0.83	0.68
True Causes (sig)	0.68	0.71	0.59	0.56	0.78	0.61	0.49	0.64	0.91	0.79	0.57	0.64	0.82	0.70	0.73	0.45
False Causes	0.13	0.31	0.17	0.23	0.06	0.13	0.23	0.35	0.05	0.16	0.29	0.34	0.03	0.13	0.20	0.35
False Causes (sig)	0.05	0.17	0.09	0.06	0.03	0.04	0.06	0.22	0.01	0.07	0.12	0.14	0.01	0.04	0.08	0.16

Table 5. Average cause support scores by an ensemble for True and False causes of a sink outcome node for random Barabasi-Albert DAGs with logistic+interaction data.

Nodes	10				20				30				40			
Sparsity	1	2	3	4	1	2	3	4	1	2	3	4	1	2	3	4
Support																
True Causes	0.84	0.74	0.69	0.68	0.80	0.71	0.67	0.68	0.86	0.83	0.67	0.71	0.80	0.75	0.78	0.67
True Causes (sig)	0.75	0.71	0.63	0.59	0.77	0.64	0.49	0.61	0.85	0.76	0.56	0.61	0.76	0.70	0.69	0.42
False Causes	0.12	0.22	0.22	0.32	0.10	0.27	0.20	0.28	0.05	0.14	0.23	0.28	0.03	0.14	0.19	0.43
False Causes (sig)	0.04	0.17	0.16	0.16	0.04	0.10	0.06	0.19	0.01	0.07	0.10	0.10	0.01	0.06	0.08	0.11

Table 6. Average cause support scores by an ensemble for True and False causes of a sink outcome node for random Barabasi-Albert DAGs with logistic data.

Nodes Sparsity Algorithm	10				20				30				40			
	0.8	1.0	1.5	2.0	0.8	1.0	1.5	2.0	0.8	1.0	1.5	2.0	0.8	1.0	1.5	2.0
FGES	0.91±0.08	0.82±0.17	0.87±0.12	0.92±0.14	0.93±0.04	0.91±0.13	0.71±0.18	0.78±0.21	0.93±0.13	0.81±0.16	0.79±0.15	0.80±0.21	0.99±0.02	0.85±0.16	0.94±0.09	0.81±0.13
HC	0.90±0.09	0.89±0.15	0.80±0.18	0.93±0.08	0.87±0.12	0.92±0.09	0.83±0.12	0.77±0.21	0.87±0.13	0.83±0.10	0.77±0.18	0.86±0.16	0.91±0.12	0.87±0.13	0.96±0.07	0.82±0.15
LINGAM	0.88±0.17	0.78±0.21	0.75±0.18	0.95±0.06	0.78±0.20	0.70±0.23	0.82±0.12	0.67±0.24	0.82±0.13	0.76±0.19	0.71±0.23	0.63±0.29	0.74±0.28	0.72±0.28	0.44±0.34	0.67±0.22
MMHC	0.89±0.10	0.88±0.15	0.84±0.15	0.89±0.13	0.88±0.10	0.92±0.09	0.84±0.12	0.84±0.13	0.89±0.10	0.83±0.09	0.77±0.19	0.87±0.15	0.95±0.09	0.88±0.15	0.95±0.08	0.81±0.15
PC	0.91±0.10	0.83±0.20	0.79±0.24	0.83±0.17	0.90±0.09	0.94±0.08	0.78±0.19	0.68±0.25	0.90±0.14	0.88±0.13	0.77±0.19	0.87±0.16	1.00±0.00	0.90±0.12	0.91±0.19	0.73±0.20
ensemble	0.91±0.08	0.88±0.17	0.90±0.10	0.91±0.12	0.90±0.09	0.93±0.08	0.84±0.11	0.84±0.15	0.94±0.07	0.84±0.10	0.81±0.16	0.87±0.16	0.96±0.09	0.88±0.14	0.95±0.08	0.85±0.13

Table 7. F1 scores for discovered causes of a sink outcome node for random Erdos-Renyi DAGs with logistic data.

Nodes Sparsity Algorithm	10				20				30				40			
	0.8	1.0	1.5	2.0	0.8	1.0	1.5	2.0	0.8	1.0	1.5	2.0	0.8	1.0	1.5	2.0
FGES	0.91±0.09	0.90±0.12	0.84±0.11	0.93±0.10	0.92±0.05	0.90±0.14	0.82±0.14	0.85±0.21	0.93±0.13	0.82±0.15	0.86±0.11	0.88±0.12	0.99±0.02	0.86±0.15	0.95±0.07	0.82±0.17
HC	0.89±0.09	0.94±0.08	0.82±0.18	0.97±0.06	0.87±0.11	0.91±0.09	0.82±0.12	0.83±0.15	0.89±0.11	0.83±0.10	0.80±0.16	0.87±0.16	0.92±0.11	0.88±0.14	0.95±0.06	0.86±0.09
LINGAM	0.80±0.24	0.76±0.19	0.73±0.18	0.96±0.07	0.80±0.16	0.65±0.24	0.76±0.12	0.70±0.25	0.80±0.15	0.76±0.19	0.67±0.24	0.70±0.24	0.74±0.26	0.71±0.28	0.69±0.32	0.67±0.21
MMHC	0.90±0.09	0.90±0.10	0.84±0.12	0.93±0.08	0.87±0.11	0.92±0.09	0.81±0.13	0.88±0.10	0.89±0.12	0.82±0.10	0.83±0.13	0.86±0.17	0.94±0.10	0.89±0.12	0.95±0.08	0.88±0.08
PC	0.90±0.11	0.82±0.21	0.69±0.24	0.70±0.29	0.91±0.08	0.91±0.11	0.79±0.18	0.70±0.31	0.88±0.16	0.88±0.10	0.86±0.12	0.80±0.23	0.99±0.02	0.88±0.14	0.89±0.19	0.72±0.24
ensemble	0.91±0.08	0.91±0.12	0.89±0.10	0.96±0.06	0.88±0.10	0.92±0.09	0.82±0.12	0.90±0.09	0.93±0.07	0.84±0.10	0.87±0.09	0.92±0.10	0.96±0.09	0.89±0.12	0.95±0.08	0.89±0.08

Table 8. F1 scores for discovered causes of a sink outcome node for random Erdos-Renyi DAGs with logistic data with pairwise interaction.

Nodes Sparsity Algorithm	10				20				30				40			
	0.8	1.0	1.5	2.0	0.8	1.0	1.5	2.0	0.8	1.0	1.5	2.0	0.8	1.0	1.5	2.0
FGES	0.89±0.10	0.91±0.09	0.80±0.13	0.87±0.14	0.86±0.09	0.71±0.26	0.73±0.19	0.82±0.17	0.83±0.16	0.75±0.22	0.72±0.17	0.81±0.20	0.99±0.04	0.80±0.20	0.91±0.16	0.77±0.14
HC	0.89±0.09	0.88±0.13	0.82±0.17	0.83±0.17	0.80±0.10	0.72±0.18	0.70±0.12	0.74±0.22	0.76±0.27	0.76±0.13	0.82±0.13	0.80±0.17	0.89±0.14	0.78±0.19	0.93±0.10	0.73±0.17
LINGAM	0.85±0.15	0.79±0.16	0.75±0.15	0.88±0.16	0.82±0.11	0.73±0.22	0.79±0.08	0.63±0.25	0.79±0.14	0.70±0.14	0.63±0.23	0.62±0.28	0.65±0.32	0.66±0.27	0.46±0.30	0.69±0.20
MMHC	0.89±0.11	0.91±0.11	0.79±0.15	0.79±0.19	0.82±0.11	0.69±0.21	0.59±0.12	0.74±0.21	0.81±0.24	0.76±0.15	0.83±0.13	0.79±0.21	0.91±0.13	0.80±0.19	0.90±0.13	0.75±0.15
PC	0.87±0.12	0.84±0.16	0.70±0.17	0.68±0.21	0.87±0.10	0.87±0.18	0.65±0.19	0.72±0.23	0.83±0.22	0.66±0.16	0.81±0.15	0.87±0.17	0.89±0.23	0.78±0.21	0.84±0.25	0.56±0.30
ensemble	0.88±0.10	0.92±0.10	0.85±0.13	0.83±0.17	0.83±0.10	0.74±0.17	0.73±0.15	0.80±0.19	0.87±0.17	0.75±0.16	0.84±0.12	0.86±0.12	0.92±0.10	0.82±0.18	0.91±0.11	0.78±0.13

Table 9. F1 scores for discovered causes of a sink outcome node for random Erdos-Renyi DAGs with linear Bernoulli data.

Nodes Sparsity Algorithm	10				20				30				40			
	1	2	3	4	1	2	3	4	1	2	3	4	1	2	3	4
FGES	0.87±0.14	0.72±0.14	0.72±0.23	0.82±0.14	0.90±0.13	0.65±0.20	0.79±0.11	0.70±0.27	0.90±0.15	0.79±0.20	0.62±0.18	0.78±0.16	0.92±0.10	0.66±0.22	0.61±0.29	0.72±0.09
HC	0.82±0.12	0.67±0.13	0.75±0.16	0.74±0.21	0.79±0.19	0.74±0.23	0.74±0.16	0.62±0.27	0.87±0.20	0.72±0.22	0.63±0.16	0.79±0.19	0.85±0.26	0.66±0.21	0.66±0.26	0.75±0.09
LINGAM	0.59±0.23	0.67±0.13	0.59±0.17	0.73±0.26	0.65±0.20	0.56±0.21	0.71±0.20	0.51±0.30	0.64±0.36	0.65±0.26	0.57±0.20	0.72±0.19	0.56±0.36	0.54±0.26	0.49±0.28	0.68±0.16
MMHC	0.78±0.12	0.69±0.11	0.79±0.13	0.75±0.20	0.82±0.16	0.70±0.18	0.73±0.12	0.61±0.24	0.90±0.17	0.74±0.23	0.64±0.15	0.81±0.17	0.84±0.28	0.75±0.18	0.67±0.23	0.75±0.09
PC	0.82±0.19	0.69±0.26	0.59±0.27	0.68±0.32	0.87±0.19	0.72±0.24	0.58±0.30	0.34±0.31	0.93±0.13	0.77±0.26	0.47±0.20	0.51±0.36	0.96±0.06	0.73±0.21	0.63±0.23	0.27±0.14
ensemble	0.88±0.14	0.78±0.10	0.77±0.15	0.76±0.20	0.88±0.13	0.73±0.17	0.78±0.08	0.64±0.27	0.91±0.16	0.78±0.17	0.68±0.12	0.80±0.18	0.90±0.14	0.78±0.18	0.71±0.20	0.73±0.09

Table 10. F1 scores for discovered causes of a sink outcome node for random Barabasi-Albert DAGs with logistic data.

Nodes Sparsity Algorithm	10				20				30				40			
	1	2	3	4	1	2	3	4	1	2	3	4	1	2	3	4
FGES	0.89±0.15	0.64±0.15	0.79±0.15	0.85±0.19	0.89±0.15	0.66±0.26	0.86±0.10	0.63±0.30	0.90±0.22	0.82±0.21	0.62±0.22	0.79±0.21	0.93±0.09	0.67±0.27	0.70±0.27	0.78±0.08
HC	0.81±0.17	0.77±0.16	0.77±0.18	0.80±0.21	0.84±0.22	0.74±0.21	0.87±0.10	0.65±0.22	0.90±0.18	0.80±0.23	0.62±0.21	0.81±0.17	0.86±0.21	0.76±0.21	0.74±0.22	0.81±0.09
LINGAM	0.60±0.22	0.64±0.11	0.58±0.13	0.70±0.27	0.59±0.19	0.54±0.21	0.70±0.18	0.51±0.29	0.64±0.35	0.60±0.27	0.54±0.19	0.74±0.18	0.67±0.30	0.51±0.22	0.50±0.27	0.69±0.13
MMHC	0.82±0.14	0.77±0.17	0.80±0.17	0.81±0.17	0.86±0.17	0.77±0.19	0.85±0.11	0.66±0.22	0.90±0.22	0.83±0.23	0.66±0.25	0.86±0.14	0.87±0.19	0.79±0.19	0.82±0.18	0.80±0.09
PC	0.70±0.29	0.66±0.23	0.67±0.31	0.66±0.37	0.90±0.14	0.69±0.26	0.47±0.33	0.41±0.35	0.94±0.12	0.80±0.29	0.54±0.25	0.49±0.34	0.89±0.23	0.74±0.24	0.68±0.21	0.35±0.23
ensemble	0.86±0.16	0.79±0.13	0.81±0.14	0.79±0.20	0.87±0.19	0.78±0.17	0.86±0.10	0.66±0.20	0.93±0.19	0.85±0.22	0.68±0.20	0.83±0.15	0.91±0.12	0.85±0.16	0.80±0.18	0.80±0.07

Table 11. F1 scores for discovered causes of a sink outcome node for random Barabasi-Albert DAGs with logistic data with pairwise interactions.

Nodes Sparsity Algorithm	10				20				30				40			
	1	2	3	4	1	2	3	4	1	2	3	4	1	2	3	4
FGES	0.91±0.13	0.74±0.13	0.82±0.17	0.79±0.14	0.76±0.26	0.62±0.22	0.80±0.07	0.59±0.28	0.86±0.24	0.83±0.17	0.60±0.19	0.82±0.15	0.91±0.12	0.66±0.21	0.68±0.27	0.76±0.07
HC	0.91±0.13	0.70±0.11	0.72±0.17	0.84±0.17	0.77±0.24	0.65±0.14	0.79±0.07	0.66±0.26	0.82±0.23	0.86±0.11	0.63±0.18	0.80±0.17	0.80±0.34	0.75±0.21	0.68±0.27	0.80±0.07
LINGAM	0.68±0.12	0.70±0.11	0.55±0.14	0.66±0.32	0.67±0.19	0.43±0.12	0.67±0.18	0.51±0.29	0.63±0.36	0.61±0.26	0.56±0.18	0.67±0.19	0.69±0.31	0.51±0.28	0.48±0.30	0.65±0.12
MMHC	0.91±0.15	0.65±0.12	0.68±0.20	0.77±0.17	0.82±0.21	0.58±0.19	0.78±0.16	0.74±0.18	0.85±0.22	0.73±0.18	0.65±0.18	0.78±0.18	0.80±0.34	0.72±0.22	0.66±0.24	0.77±0.09
PC	0.76±0.33	0.84±0.12	0.69±0.24	0.68±0.32	0.89±0.13	0.79±0.09	0.57±0.32	0.50±0.39	0.88±0.26	0.82±0.29	0.66±0.18	0.52±0.33	0.83±0.31	0.76±0.20	0.67±0.31	0.41±0.24
ensemble	0.91±0.15	0.77±0.10	0.76±0.18	0.77±0.18	0.82±0.23	0.63±0.14	0.80±0.10	0.72±0.20	0.87±0.20	0.89±0.10	0.69±0.16	0.81±0.14	0.83±0.28	0.76±0.20	0.72±0.23	0.77±0.08

Table 12. F1 scores for discovered causes of a sink outcome node for random Barabasi-Albert DAGs with linear Bernoulli data.

Sensitivity to effect size and sample sizes (potential unfaithfulness). The constraints in the Bernoulli linear data generation mechanism may produce weights of small magnitude (i.e., low effect size). Figure 8 shows CSL algorithms have relatively poor performance for the ER model with Bernoulli linear data generation. However, for the BA model, the performance is similar for all three data generation options. The experimental setup used to assess whether CSL algorithms are sensitive to probable unfaithfulness caused by a small number of samples is described next. We generate 100 random DAGs consisting of $n = 30$ nodes with an edge sparsity of 2 for both the ER and BA models. Then, for each DAG, we evaluate the ensemble of five algorithms described above with sample sizes of $n \times 25$, $n \times 50$, $n \times 100$, and $n \times 500$. Table 13 and Figure 9 summarize the results of this experiment. For limited samples, the CSL algorithms are more likely to miss the true causes, and the average support for the true causes is lower. Thus, a majority voting ensemble suffers due to limited samples. A ranking scheme utilizing cause support, magnitude of causal effects, and significance support may be more preferable than a threshold voting scheme. The results for real-world applications in the main paper follow this ranking scheme.

Topology Samples Support	BA								ER
	$n \times 25$	$n \times 50$	$n \times 100$	$n \times 500$	$n \times 25$	$n \times 50$	$n \times 100$	$n \times 500$	$n \times 500$
True Causes	0.56	0.62	0.66	0.75	0.44	0.53	0.60	0.72	0.72
True Causes (sig)	0.45	0.51	0.55	0.65	0.35	0.42	0.48	0.61	0.61
False Causes	0.11	0.13	0.14	0.17	0.07	0.12	0.14	0.15	0.15
False Causes (sig)	0.02	0.03	0.04	0.06	0.02	0.02	0.03	0.05	0.05

Table 13. Sensitivity of average cause support to potential unfaithfulness due to limited sample size for $n = 30$, and $sp_{ba} = sp_{er} = 2$. For limited samples, CSL algorithms may miss true causes as well. A ranking scheme utilizing cause support, magnitude of causal effects, and significance support may be more favorable than a voting ensemble.

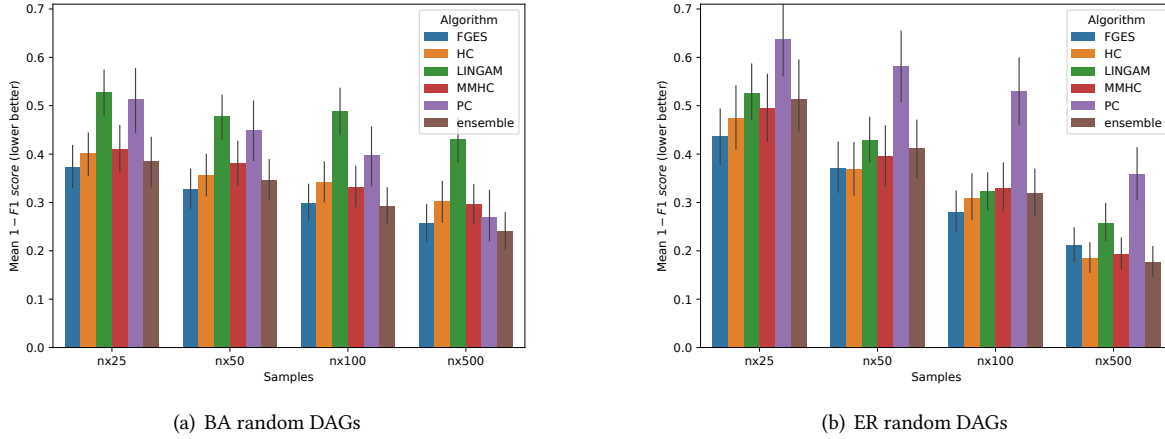


Fig. 9. Sensitivity of CSL algorithms to potential unfaithfulness due to limited sample size ($n=30$ nodes, sparsity=2). Ranking causes according to cause support, magnitude of effects, and significance support should be prioritized over a (majority) voting ensemble for robustness.

Ranking causes. Here, we present the procedure for summarizing risk factors or preventive factors of a repeated undesirable outcome, as shown in Figure 6. Our framework outputs a list of causes with two properties associated with each cause: cause support ($S_c(X^j)$) and multi-set of total causal effects $\mathbf{T}(X^j) := \{\forall k \in \{1, \dots, K\}, X_{CATE}^j(Z = \emptyset) \text{ if } (X^j, G_k) \in \mathbf{R} \text{ else } 0\}$. For generating top risk factors, the causes are ranked in the descending order of cause support $S_c(X^j)$ as a primary sort key and the descending order of maximum causal effect in a multi-set, i.e. $\max(\mathbf{T}(X^j))$, as a secondary sort key. The top N risk factors are displayed according to descending order of $\max(\mathbf{T}(X^j))$. The stacked bars show the multi-set effects with lower values overlapping the higher values. For generating top preventive factors, the secondary sort is done in the ascending order of minimum causal effect in a multi-set, i.e. $\min(\mathbf{T}(X^j))$. The top N preventive factors are displayed according to the ascending order of $\min(\mathbf{T}(X^j))$. This procedure generalizes to the effect modifier analysis, as depicted in Figure 5, where heterogeneous causal effects are considered instead of total causal effects.

Orienting Undirected Edges

Orientation support. The undirected edges due to the equivalence class of a DAG are oriented utilizing the temporal order of events prominent across population \mathbf{P} in the event-log data model. We define *orientation support* for an edge direction from V_j to V_k $V_j \rightarrow V_k$ as $S_o(j, k) = \frac{1}{n(\mathbf{D})} \sum_{i \in \mathbf{D}} \llbracket \min(t|e_{i,t}^j = 1) < \min(t|e_{i,t}^k = 1) \rrbracket$, where $\mathbf{D} \subseteq \mathbf{P} := \{E_i | \exists p, e_{i,p}^j = 1 \wedge \exists q, e_{i,q}^k = 1\}$ is subpopulation with both events e^j and e^k in a timeline E_i and $\llbracket \cdot \rrbracket$ is an indicator function. $S_o(j, k)$ gives the fraction of units with the parent event e^j before the child event e^k for a given edge orientation. We calculate $S_o(j, k)$ for all the possible orientations of undirected edges, sort the edges from highest to lowest support, and orient the edges by handling the constraints of no cycles and no new v-structures to obtain one DAG per CSL algorithm.

Algorithm 1 shows our greedy approach of orienting undirected edges for any causal structure learning (CSL) algorithm that outputs an equivalence class of a DAG. The input to Algorithm 1 is a set of edges \mathbf{E} where direction can be a null value for undirected edges and the output is a set of edges \mathbf{D} without null direction. First, we calculate $S_o(j, k)$, defined in the Methodology Section, for all the possible orientations of undirected edges (lines

5-6). The undirected and directed edges are stored to \mathbf{U} and \mathbf{D} respectively (line 7-9). Second, we sort the edge orientations from highest to lowest support (line 12). Finally, we orient the edges by handling the constraints of no cycles and no new unshielded v-structures to obtain one DAG per CSL algorithm (lines 13-26).

Algorithm 1 Orienting undirected edges.

 Input: \mathbf{E} , Output: \mathbf{D}

```

1:  $\mathbf{S} \leftarrow \{\}$ 
2:  $\mathbf{D} \leftarrow \{\}$ 
3:  $\mathbf{U} \leftarrow \{\}$ 
4: for  $(V_j, direction, V_k) \in \mathbf{E}$  do
5:   if  $direction = \emptyset$  then
6:      $\mathbf{S} \leftarrow \mathbf{S} \cup \{(V_j, V_k, S_o(j, k)), (V_k, V_j, S_o(k, j))\}$ 
7:      $\mathbf{U} \leftarrow \mathbf{U} \cup \{(V_j - V_k)\}$ 
8:   else
9:      $\mathbf{D} \leftarrow \mathbf{D} \cup \{(V_j \xrightarrow{direction} V_k)\}$ 
10:  end if
11: end for
12:  $\mathbf{S} \leftarrow \text{sort\_desc}(\mathbf{S}, \text{key} = S_o(j, k) \in (V_j, V_k, S_o(j, k)))$ 
13: for  $(V_j, V_k, S_o(j, k)) \in \mathbf{S}$  do
14:   if  $(V_k \rightarrow V_j) \in \mathbf{D}$  then
15:     goto continue
16:   end if
17:    $G \leftarrow \text{graph}(\mathbf{D} \cup \mathbf{U})$ 
18:    $\mathbf{P} \leftarrow \text{pa}(V_k, G)$ 
19:   if  $n(\mathbf{P}) > 0 \wedge \exists V_i \in \mathbf{P}, \neg \text{adj}(V_j, V_i, G)$  then
20:     goto continue
21:   end if
22:    $\mathbf{N} = \{(V_j \rightarrow V_k)\} \cup \text{Meek95}((V_j \rightarrow V_k), G)$ 
23:    $\mathbf{D} \leftarrow \mathbf{D} \cup \mathbf{N}$ 
24:    $\mathbf{U} \leftarrow \mathbf{U} \setminus \text{undirected}(\mathbf{N})$ 
25:   continue:
26: end for

```

We iterate through all the possible ordered orientations and add new edge orientations to the set of edges (lines 22-23) if there are no conflicts. Lines 14 to 16 check the cycle due to the edges already oriented in the reverse direction in prior iterations. A new unshielded v-structure is introduced if, for a proposed orientation, the child node already has other parents that are not adjacent to the proposed parent in the current graph G (line 17-19). The addition of such an orientation is skipped (line 20).

The addition of a new orientation is followed by orientation of the graph G according to the rules by Meek [33] (line 22). The implementation of orientation using Meek [33] rules is available via `pcalg`¹ package [43]. The resulting output DAG contains all the edges in \mathbf{D} . Algorithm 1 uses the orientation order as heuristics to orient the undirected edges of an equivalence class, and ensures soundness by not introducing any new edge, cycle, or unshielded collider, as well as not deleting any undirected edge. While the above algorithm ensures scalability, a brute force implementation by enumerating all valid orientations and selecting orientation with maximum orientation support is more suitable for a few undirected edges.

¹<https://cran.r-project.org/web/packages/pcalg/index.html>

Experimental Setup

Here, we first specify our computing infrastructure along with additional software packages used in the experiments. Then, we describe the hyperparameters of the five causal structure learning algorithms considered in the experiments: MMHC, HC, FGES, PC, and LINGAM.

Computing infrastructure. We run our experiments on a device with 64-cores CPU (AMD Opteron(TM) Processor 6274 model), 118 GB RAM, 4 TB HDD, and Ubuntu 18.04 operating system. We use Anaconda² for Python package and virtual environment management. We use the bnlearn package with R version 4.0.3 for implementing HC and MMHC algorithms. For the implementation of LINGAM algorithm, we use R's pcalg package. The FGES and PC algorithms are implemented using py-causal package which is a Python wrapper for Java-based Tetrad³ package for causal structure learning. We use another virtual environment with Python 3.7.

We utilize Python's networkx package for graph processing and statsmodels package for regression and non-parametric estimation of causal effects. Python packages pandas and numpy are used for data generation, cleaning and processing, while matplotlib and seaborn packages are used for visualization. Our code and semi-synthetic dataset will be publicly available after publication.

Hyperparameters. We first describe the hyperparameters for the discrete version of the FGES algorithm available with py-causal package. FGES uses a BDeu (Bayesian Dirichlet likelihood equivalence and uniform) [20] as a scoring function that ensures the same dependence and independence relations get the same score. Other parameters and their values are as follows.

- `priorKnowledge={forbidirect:{ $\forall j \in \{1, \dots, M\}, (Y \rightarrow X^j)$ }}`, a dictionary with values containing a set of restricted edges according to the structural constraints defined in the Methodology Section.
- `dataType="discrete"`, specifies we have discrete data.
- `faithfulnessAssumed=False`, specifies data distribution may violate the faithfulness assumption, and a robust implementation should be used.
- `maxDegree = -1`, specifies no assumptions on the sparsity of the underlying causal graph and no restriction on the maximum degree of the output graph.
- `symmetricFirstStep=True`, a setting recommended in the documentation for discrete causal structure search.

PC algorithm uses `priorKnowledge` and `dataType` similar to the FGES algorithm. We set the following hyperparameters and leave all other parameters as default.

- `testId="chi-square-test"`, conditional independence test for categorical variables.
- `concurrentFAS=True`, use parallized fast adjacency search.
- `depth=5`, maximum number of conditioning set (ensuring algorithm runs in reasonable time).
- `conflictRule=2`, if conflicts arises in collider discovery, then orient conflict as bidirected edge like FCI algorithm.
- `colliderDiscoveryRule=3`, collider orientation by choosing the separation-sets with the maximum p-value. Robust for small sample sizes.

For the HC algorithm, we set the following hyperparameters and leave all other parameters as default.

- `score="bic"` (default), specifies BIC (Bayesian Information Criterion) [9] scoring function.
- `maxp=Inf` (default), specifies the maximum number of parents in the output graph and is equivalent to `maxDegree` parameter for FGES.

²<https://www.anaconda.com/>

³<http://cmu-phil.github.io/tetrad/manual/>

- `blacklist` = $\{\forall j \in \{1, \dots, M\}, (Y \rightarrow X^j)\}$, a dataframe format with columns `from` and `to` that specifies the forbidden edges.

We use all the default parameters for the hybrid MMHC algorithm except for the `blacklist` parameter that specifies the same structural constraints used for HC. The constraint-based MMPC algorithm within MMHC uses mutual information for conditional independence tests, `alpha=0.05` that specifies type I error rate for the statistical test, and `max.sx = Inf` that indicates an unrestricted conditioning set. We use the default parameters for LINGAM.